

OPEN ACCESS

Performance of τ -lepton reconstruction and identification in CMS

To cite this article: CMS Collaboration 2012 *JINST* **7** P01001

View the [article online](#) for updates and enhancements.

Related content

- [Performance of the CMS drift-tube chamber local trigger with cosmic rays](#)
CMS Collaboration
- [Performance of CMS hadron calorimeter timing and synchronization using test beam, cosmic ray, and LHC beam data](#)
CMS Collaboration
- [Performance study of the CMS barrel resistive plate chambers with cosmic rays](#)
CMS Collaboration

Recent citations

- [Search for third-generation scalar leptoquarks decaying to a top quark and a \$\tau\$ lepton at \$\sqrt{s}=13\$ TeV](#)
A. M. Sirunyan *et al*
- [Performance of reconstruction and identification of leptons decaying to hadrons and \$\nu\$ in pp collisions at \$\sqrt{s}=13\$ TeV](#)
A.M. Sirunyan *et al*
- [Search for Higgs boson pair production in the \$b\bar{b}\$ final state in proton-proton collisions at \$\sqrt{s}=8\$ TeV](#)
A. M. Sirunyan *et al*

**IOP | ebooks™**

Bringing you innovative digital publishing with leading voices to create your essential collection of books in STEM research.

Start exploring the collection - download the first chapter of every title for free.

LHC REFERENCE VOLUME

Performance of τ -lepton reconstruction and identification in CMS

CMS collaboration

ABSTRACT: The performance of τ -lepton reconstruction and identification algorithms is studied using a data sample of proton-proton collisions at $\sqrt{s} = 7$ TeV, corresponding to an integrated luminosity of 36 pb^{-1} collected with the CMS detector at the LHC. The τ leptons that decay into one or three charged hadrons, zero or more short-lived neutral hadrons, and a neutrino are identified using final-state particles reconstructed in the CMS tracker and electromagnetic calorimeter. The reconstruction efficiency of the algorithms is measured using τ leptons produced in Z-boson decays. The τ -lepton misidentification rates for jets and electrons are determined.

KEYWORDS: Si microstrip and pad detectors; Calorimeter methods; Detector modelling and simulations I (interaction of radiation with matter, interaction of photons with matter, interaction of hadrons with matter, etc)

Contents

1	Introduction	1
2	CMS detector	2
3	CMS τ_h reconstruction algorithms	3
3.1	HPS algorithm	3
3.2	TaNC algorithm	5
4	Efficiency of τ_h reconstruction and identification	5
5	Reconstruction of the τ_h decay mode	8
6	Reconstruction of the τ_h energy	10
7	Measurement of the τ_h misidentification rate for jets	10
8	Measurement of the τ_h misidentification rate for electrons	13
9	Summary	14
	The CMS collaboration	17

1 Introduction

The primary goal of the Compact Muon Solenoid (CMS) [1] experiment is to explore particle physics at the TeV energy scale by studying the final states produced in the proton-proton collisions at the Large Hadron Collider (LHC) [2]. Leptons play a very important role in these studies because they often represent an experimentally favourable signature.

The three generations of charged leptons, electrons, muons, and taus, are characterized by their masses. Because of their higher mass, τ leptons play a crucial role in the searches for the standard model (SM) Higgs boson, especially for the mass region below twice the W-boson mass. The motivation for searches for the Higgs boson in its τ -leptonic decays is also supported for example by the minimal supersymmetric standard model (MSSM) [3]. Other models of new physics, such as supersymmetric left-right models (SUSYLR), also predict increased couplings to the third-generation charged fermions. As a result, the decay chains of the supersymmetric particles lead to the lighter stau, which can lead to multi-tau final states [4]. Lepton universality ensures that one third of W and Z-boson leptonic decays result in τ leptons. When measuring rare processes, this contribution becomes substantial. For example, in the search for high-mass SM Higgs bosons that decay preferentially into W and Z bosons, the addition of modes with τ leptons in the final state improves the early discovery potential.

The lifetime of τ leptons is short enough that they decay before reaching the detector elements. In two thirds of the cases, τ leptons decay hadronically, typically into one or three charged mesons (predominantly π^+ , π^-), often accompanied by neutral pions (decaying via $\pi^0 \rightarrow \gamma\gamma$), and a ν_τ .

The CMS collaboration has designed algorithms that use final-state photons and charged hadrons to identify hadronic decays of τ leptons (τ_h) through the reconstruction of the intermediate resonances. The ν_τ escapes undetected and is not considered in the τ_h reconstruction. These algorithms use decay mode identification techniques and efficiently discriminate against potentially large backgrounds from quarks and gluons that occasionally hadronize into jets of low particle multiplicity. The algorithms described here have already been successfully used in a measurement of the $Z \rightarrow \tau\tau$ production cross section [5] and in a search for neutral MSSM Higgs bosons decaying into τ pairs [6].

This paper describes performance studies based on a sample of proton-proton collisions collected during 2010 at $\sqrt{s} = 7$ TeV, corresponding to an integrated luminosity of 36 pb^{-1} . The analysis uses genuine taus from inclusive $Z \rightarrow \tau\tau$ production. One tau is required to decay leptonically, into a muon, and the other one hadronically, thus creating a $\mu\tau_h$ final state. The analysis provides estimates of the τ_h reconstruction and identification efficiency, and determines the misidentification rate, the probability for quark and gluon jets or electrons to be misidentified as τ_h . This paper uses the selection requirements that are most commonly used in the Z and Higgs analyses, and compares the LHC collision data with predictions based on Monte Carlo (MC) simulation.

2 CMS detector

A detailed description of CMS can be found elsewhere [1]. The central feature of the CMS apparatus is a superconducting solenoid of 6 m internal diameter, providing a magnetic field of 3.8 T. Within the field volume are the silicon pixel and strip tracker, the crystal electromagnetic calorimeter (ECAL), and the brass/scintillator hadron calorimeter (HCAL). Muons are measured in gas-ionization detectors embedded in the steel return yoke.

CMS uses a right-handed coordinate system, with the origin at the nominal interaction point, the x axis pointing to the centre of the LHC ring, the y axis pointing up perpendicular to the LHC plane, and the z axis along the counterclockwise beam direction. The polar angle θ is measured from the positive z axis and the azimuthal angle ϕ is measured in the x - y plane. Variables used in this article are the pseudorapidity, $\eta \equiv -\ln[\tan(\theta/2)]$, and the transverse momentum, $p_T = \sqrt{p_x^2 + p_y^2}$.

The ECAL is designed to have both excellent energy resolution and high granularity, properties that are crucial for reconstructing electrons and photons produced in τ -lepton decays. The ECAL is constructed with projective lead tungstate crystals in two pseudorapidity regions: the barrel ($|\eta| < 1.479$) and the endcap ($1.479 < |\eta| < 3$). In the barrel region, the crystals are $25.8X_0$ long, where X_0 is the radiation length, and provide a granularity of $\Delta\eta \times \Delta\phi = 0.0174 \times 0.0174$. The endcap region is instrumented with a lead/silicon-strip preshower detector consisting of two orthogonal strip detectors with a strip pitch of 1.9 mm. One plane is at a depth of $2X_0$ and the other at $3X_0$. The ECAL has an energy resolution of better than 0.5% for unconverted photons with transverse energies above 100 GeV.

Table 1. Branching fractions of the dominant hadronic decays of the τ lepton and the symbol and mass of any intermediate resonance [9]. The h stands for both π and K , but in this analysis the π mass is assigned to all charged particles. The table is symmetric under charge conjugation.

Decay mode	Resonance	Mass (MeV/c ²)	Branching fraction (%)
$\tau^- \rightarrow h^- \nu_\tau$			11.6%
$\tau^- \rightarrow h^- \pi^0 \nu_\tau$	ρ^-	770	26.0%
$\tau^- \rightarrow h^- \pi^0 \pi^0 \nu_\tau$	a_1^-	1200	9.5%
$\tau^- \rightarrow h^- h^+ h^- \nu_\tau$	a_1^-	1200	9.8%
$\tau^- \rightarrow h^- h^+ h^- \pi^0 \nu_\tau$			4.8%

The inner tracker measures charged particle tracks within the range $|\eta| < 2.5$. It consists of 1440 silicon pixel and 15148 silicon strip detector modules, and provides an impact parameter resolution of $\sim 15 \mu\text{m}$ and a transverse momentum resolution of about 1.5% for 100 GeV particles. The reconstructed tracks are used to measure the location of interaction vertex(es). The spatial resolution of the reconstruction is $\approx 25 \mu\text{m}$ for vertexes with more than 30 associated tracks [7].

The muon barrel region is covered by drift tubes, and the endcap regions by cathode strip chambers. In both regions, resistive plate chambers provide additional coordinate and timing information. Muons can be reconstructed in the range $|\eta| < 2.4$, with a typical p_T resolution of 1% for $p_T \approx 40 \text{ GeV}/c$.

3 CMS τ_h reconstruction algorithms

CMS has developed two algorithms for identifying τ_h decays, based on the categorization of the τ_h -decay channels through the reconstruction of intermediate resonances: the hadron plus strips (HPS) and the tau neural classifier (TaNC) algorithms. The HPS algorithm is used as the main algorithm in most previous CMS τ analyses, with TaNC used for crosschecks. Both algorithms use particle flow (PF [8]) particles. In the PF approach, information from all subdetectors is combined to reconstruct and identify all particles produced in the collision. The particles are classified into mutually exclusive categories: charged hadrons, photons, neutral hadrons, muons, and electrons. These algorithms are designed to optimize the performance of the τ_h identification and reconstruction by considering the different hadronic decay modes of the tau individually. The dominant hadronic decays of τ leptons consist of one or three charged π mesons and up to two π^0 mesons, as summarized in table 1.

Both algorithms start the reconstruction of a τ_h candidate from a PF jet, whose four-momentum is reconstructed using the anti- k_T algorithm with a distance parameter $R = 0.5$ [10]. Using a PF jet as an initial seed, the algorithms first reconstruct the π^0 components of the τ_h , then combine them with charged hadrons to reconstruct the tau decay mode and calculate the tau four-momentum and isolation quantities.

3.1 HPS algorithm

The HPS algorithm gives special attention to photon conversions in the CMS tracker material. The bending of electron/positron tracks in the magnetic field of the CMS solenoid broadens the calorimeter signatures of neutral pions in the azimuthal direction. This effect is taken into account in the

HPS algorithm by reconstructing photons in “strips”, objects that are built out of electromagnetic particles (PF photons and electrons). The strip reconstruction starts by centering a strip on the most energetic electromagnetic particle within the PF jet. The algorithm then searches for other electromagnetic particles within a window of size $\Delta\eta = 0.05$ and $\Delta\phi = 0.20$ centered on the strip center. If other electromagnetic particles are found within that window, the most energetic one gets associated with the strip and the strip four-momentum is recalculated. The procedure is repeated until no further particles are found that can be associated with the strip. Strips satisfying a minimum transverse momentum requirement of $p_T^{\text{strip}} > 1 \text{ GeV}/c$ are finally combined with the charged hadrons to reconstruct individual τ_h decay modes.

The decay topologies that are considered by the HPS tau identification algorithm are

1. *Single hadron* corresponds to $h^- \nu_\tau$ and $h^- \pi^0 \nu_\tau$ decays in which the neutral pions have too little energy to be reconstructed as strips.
2. *One hadron + one strip* reconstructs the decay mode $h^- \pi^0 \nu_\tau$ in events in which the photons from π^0 decay are close together on the calorimeter surface.
3. *One hadron + two strips* corresponds to the decay mode $h^- \pi^0 \nu_\tau$ in events in which photons from π^0 decays are well separated.
4. *Three hadrons* corresponds to the decay mode $h^- h^+ h^- \nu_\tau$. The three charged hadrons are required to come from the same secondary vertex.

There are no separate decay topologies for the $h^- \pi^0 \pi^0 \nu_\tau$ and $h^- h^+ h^- \pi^0 \nu_\tau$ decay modes. They are reconstructed via the existing topologies. All charged hadrons and strips are required to be contained within a cone of size $\Delta R = (2.8 \text{ GeV}/c)/p_T^{\tau_h}$, where $p_T^{\tau_h}$ is the transverse momentum of the τ_h as reconstructed by HPS. The reconstructed tau momentum \vec{p}^{τ_h} is required to match the (η, ϕ) direction of the original PF jet within a maximum distance of $\Delta R = 0.1$, where $\Delta R = \sqrt{(\Delta\eta)^2 + (\Delta\phi)^2}$.

The four-momenta of charged hadrons and strips are reconstructed according to the respective τ_h decay topology hypothesis, assuming all charged hadrons to be pions, and are required to be consistent with the masses of the intermediate meson resonances listed in table 1. The following invariant mass windows are allowed for candidates: $50\text{--}200 \text{ MeV}/c^2$ for π^0 , $0.3\text{--}1.3 \text{ GeV}/c^2$ for ρ , and $0.8\text{--}1.5 \text{ GeV}/c^2$ for a_1 . In cases where a τ_h decay is consistent with more than one hypothesis, the hypothesis giving the highest $p_T^{\tau_h}$ is chosen.

Finally, reconstructed candidates are required to be isolated. The isolation criterion requires that, apart from the τ_h decay products, there be no charged hadrons or photons present within an isolation cone of size $\Delta R = 0.5$ around the direction of the τ_h . By adjusting the p_T threshold for particles that are considered in the isolation cone, three working points, “loose”, “medium”, and “tight” are defined. The working points are determined using a simulated sample of QCD dijet events. The “loose” working point corresponds to a probability of approximately 1% for jets to be misidentified as τ_h . Successive working points reduce the misidentification rate by a factor of two with respect to the previous one.

3.2 TaNC algorithm

In the TaNC case the leading (highest- p_T) particle is required to have a p_T above 5 GeV/ c and to be within $\Delta R = 0.1$ around the jet direction. The PF τ_h four-momentum is reconstructed as a sum of the four-momenta of all particles with p_T above 0.5 GeV/ c in a cone of radius $\Delta R = 0.15$ around the direction of the leading particle. A signal cone size is defined to be $\Delta R_{\text{photons}} = 0.15$ for photons and $\Delta R_{\text{charged}} = (5 \text{ GeV})/E_T$ for charged hadrons, where E_T is the transverse energy of the PF τ_h , and $\Delta R_{\text{charged}}$ is restricted to be within the range $0.07 \leq \Delta R_{\text{charged}} \leq 0.15$. The signal cone is the region where the τ_h decay products are expected to be found. An isolation annulus is defined between the signal cone and a wider isolation cone of outer radius $\Delta R = 0.5$ around the leading particle.

The decay mode is reconstructed from the particles that are contained within the signal cone of the τ_h candidate by counting the number of tracks and π^0 meson candidates. The π^0 meson candidates are reconstructed by merging pairs of photons that have an invariant mass of less than 0.2 GeV/ c^2 . All unpaired photons are considered as π^0 candidates if their p_T exceeds 10% of the PF τ_h transverse momentum.

The decay mode of each τ_h candidate is uniquely determined by the multiplicity of reconstructed objects in the signal cone. Candidates with decay topologies other than those listed in table 1 are immediately rejected. Otherwise, a neural network is used to compute a discriminant quantity for the τ_h candidate. Each decay mode of table 1 uses a different neural network. The input observables used for each neural network are optimized for the topology of the decay mode, and are constructed from the four-momenta of the particles in the signal cone and the isolation annulus. In general, the signal cone input observables are chosen to parameterize the decay kinematics of the intermediate resonance, and the isolation cone observables to describe the multiplicity and p_T spectrum of nearby particles. The variables include angular correlations between different particles within the signal and the isolation cones, invariant masses calculated using different combinations of the particles, transverse momenta, and numbers of charged particles in the signal and the isolation regions. The neural networks are trained to discriminate between genuine τ_h produced in $Z \rightarrow \tau\tau$ decays and misidentified jets from a sample of QCD multijet events. The set of input observables for a given neural network is chosen to be the minimal set of observables for which the removal of any two input variables significantly degrades the classification performance.

The output of the neural network is a continuous quantity. By adjusting the thresholds of selections on the neural network output, three working points, again called “loose”, “medium”, and “tight”, are defined, similar to those discussed in section 3.1.

4 Efficiency of τ_h reconstruction and identification

To compare the performance of τ_h reconstruction in data and MC simulation, a set of MC samples is used to reproduce a mixture of signal and background events. The signal is expected to come from inclusive $Z \rightarrow \tau\tau$ production. The major sources of background are QCD multijet, W production with associated jets, $\mu\mu$ Drell–Yan production, and $t\bar{t}$ production. The Drell–Yan signal and background are simulated with the next-to-leading order (NLO) MC generator POWHEG [11–13]. The QCD multijet and W backgrounds are simulated with PYTHIA [14] and the top quark samples with Madgraph [15]. The τ -lepton decays are simulated with Tauola [16]. The samples

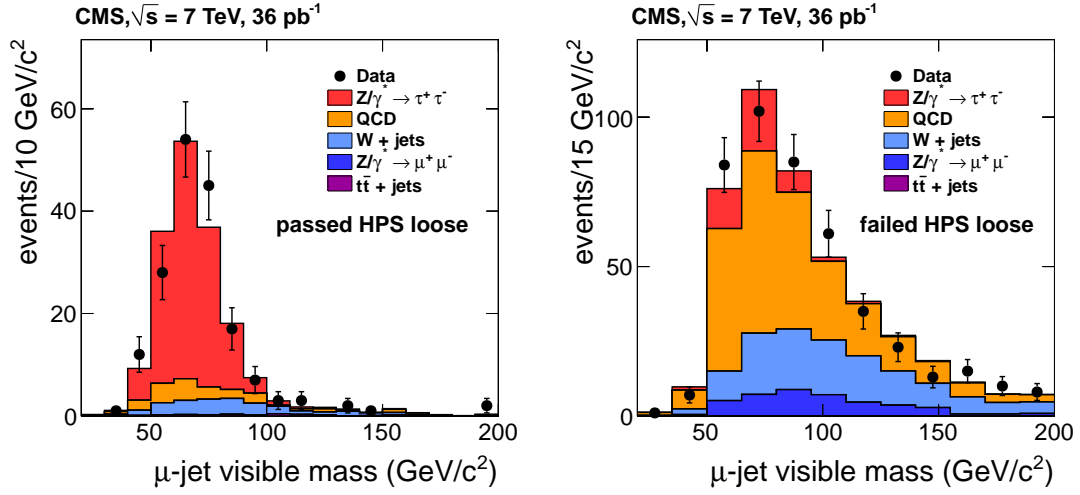


Figure 1. Invariant mass distribution of the μ -jet system for preselected events which pass (left) and fail (right) the HPS “loose” τ_h identification requirements (solid symbols) compared to predictions of the MC simulation (histograms).

are normalized using the cross section at next-to-next-to-leading order (NNLO) for Drell–Yan and W, at leading order (LO) for QCD, and NLO for the $t\bar{t}$ sample. The MC samples are mixed based on the corresponding cross sections.

To measure the efficiency of τ_h reconstruction and identification in data, a tag-and-probe method is used with a sample of $Z \rightarrow \tau\tau \rightarrow \mu\tau_h$ events. The events are preselected using kinematic cuts and a set of requirements to suppress the background from $Z \rightarrow \mu\mu$, W, and QCD events, but without applying the τ_h -identification algorithms. The preselection requires the event to be triggered by a single-muon high level trigger [17], and to contain only one isolated muon with $p_T^\mu > 15 \text{ GeV}/c$ within the geometric acceptance $|\eta_\mu| < 2.1$, that is used as a tag. An isolated jet candidate of $p_T^{\text{jet}} > 20 \text{ GeV}/c$ within the geometric acceptance $|\eta_{\text{jet}}| < 2.3$, with a “leading” (highest- p_T) track constituent in the jet with $p_T > 5 \text{ GeV}/c$, is used as a probe. The preselection is needed to increase the percentage of $Z \rightarrow \tau\tau$ events in the final sample. This preselection clearly biases the sample, but the bias is taken into account when computing the final efficiency. The muon and the “leading” track in the jet are required to be of opposite charge. To suppress background from W+jet(s) events, an additional requirement on transverse mass, M_T , of the muon and missing transverse energy, E_T^{miss} , of less than 40 GeV is applied. The transverse mass is defined as $M_T = \sqrt{2p_T^\mu E_T^{\text{miss}} \cdot (1 - \cos\Delta\phi)}$, where p_T^μ is the muon transverse momentum and $\Delta\phi$ is the azimuthal angle between the E_T^{miss} vector and p_T^μ .

The HPS and TaNC algorithms are both applied to the preselected events. The resulting invariant mass distributions of the μ -jet system for those events that pass or fail the τ_h identification are fitted using signal and background distributions provided by MC simulation. The efficiency is then calculated as $\varepsilon = N_{\text{pass}}^{Z \rightarrow \tau\tau} / (N_{\text{pass}}^{Z \rightarrow \tau\tau} + N_{\text{fail}}^{Z \rightarrow \tau\tau})$, where $N_{\text{pass,fail}}^{Z \rightarrow \tau\tau}$ are the numbers of $Z \rightarrow \tau\tau$ events after background contributions are subtracted. Figure 1 shows the invariant mass of the μ -jet system for preselected events that pass (left) and fail (right) the “loose” τ_h identification requirements.

Table 2. Efficiency for a τ_h to pass the HPS and TaNC identification criteria, measured by fitting the $Z \rightarrow \tau\tau$ signal contribution in the samples of the “passed” and “failed” preselected events. The uncertainties of the fit are statistical only. The statistical uncertainties of the MC predictions are small and can be neglected. The last column represents the data-to-MC correction factors and their full uncertainties including statistical and systematic components. Data-to-MC ratios for the τ_h reconstruction efficiency determined using fits to the measured Z production cross sections as described in [5] are also shown.

Algorithm	Fit data	Expected MC	Data/MC
HPS “loose”	0.70 ± 0.15	0.70	1.00 ± 0.24
HPS “medium”	0.53 ± 0.13	0.53	1.01 ± 0.26
HPS “tight”	0.33 ± 0.08	0.36	0.93 ± 0.25
TaNC “loose”	0.76 ± 0.20	0.72	1.06 ± 0.30
TaNC “medium”	0.63 ± 0.17	0.66	0.96 ± 0.27
TaNC “tight”	0.55 ± 0.15	0.55	1.00 ± 0.28
HPS “loose”	$\tau\tau$ combined fit [5]		0.94 ± 0.09
HPS “loose”	$\tau\tau$ to $\mu\mu, ee$ fit [5]		0.96 ± 0.07

Since in the “failed” sample there is no τ_h reconstructed, for consistency the visible mass is always computed using the jet four-vector and not the four-vector as reconstructed by the τ_h algorithms. The MC predictions for signal and background events are also shown. The “passed” sample is dominated by Z events and a small background contribution. The sample of “failed” events is dominated by background contributions. The MC predictions describe the data reasonably well. The stability of the fit results is tested by using background estimates from data instead of the MC predictions and by varying the invariant mass ranges for the fit. All checks demonstrate consistent results within the uncertainties of the method.

Results of the fits are summarized in table 2. The values measured in data, “Fit data”, are compared with the expected values, “Expected MC”, obtained by repeating the fitting procedure on simulated events. The background and signal normalizations correspond to the best fit. The efficiency of the τ_h algorithms on preselected events is approximately 30% higher than for an inclusive sample, without preselection. In general the value of the efficiency depends on the p_T and η requirements, which are applied in each individual physics analysis. The main goal of this study is to perform the data-to-MC comparison and to determine data-to-MC correction factors and their uncertainties. The agreement in the mean values of the fits between data and MC simulation is observed to be better than a few percent, although with this data sample, the statistical uncertainties of the fits are in the range of 20–30%.

Systematic uncertainties on the measured τ_h identification efficiencies that are not taken into account by the fit procedure arise from uncertainties on track reconstruction (4%) and from uncertainties on the probabilities for jets to pass the “leading” track p_T and loose isolation requirements applied in the preselection ($\leq 12\%$). Uncertainties on track momentum and τ_h energy scales have an effect on the measured τ_h identification efficiencies below 1%. All numbers represent relative uncertainties.

The resulting ratio of the measured efficiencies to those predicted by MC simulation for τ_h decays to pass the “loose”, “medium”, and “tight” HPS and TaNC working points are presented in the last column of table 2. The uncertainties on the ratios represent the full uncertainties of the

Table 3. The expected efficiency for τ_h decays to pass the HPS and TaNC identification criteria estimated using $Z \rightarrow \tau\tau$ events selected for analyses from the MC simulation for two different selection requirements on $p_T^{\tau_h}$. The requirement is applied both at the reconstruction and generator levels. The statistical uncertainties of the MC predictions are smaller than the least significant digit of the efficiency values in the table and are not shown.

Algorithm	HPS			TaNC		
	“loose”	“medium”	“tight”	“loose”	“medium”	“tight”
Efficiency ($p_T^{\tau_h} > 15 \text{ GeV}/c$)	0.46	0.34	0.23	0.54	0.43	0.30
Efficiency ($p_T^{\tau_h} > 20 \text{ GeV}/c$)	0.50	0.37	0.25	0.58	0.48	0.36

method, which are calculated by adding the statistical and systematic uncertainties in quadrature. The total uncertainty of the measured efficiency of the τ_h algorithms is dominated by the statistical uncertainty of the fit. The simulation describes the data well. Since the same event sample is used to evaluate efficiencies for different working points, the results are correlated.

The values presented in table 2 are used as inputs for fits to measure the uncertainty of the τ_h reconstruction and identification efficiency with higher precision by comparing the yield of the $Z \rightarrow \tau\tau$ events in different decay modes and the yield of $Z \rightarrow \mu\mu$ and $Z \rightarrow ee$ events, as described elsewhere [5]. The first approach uses a simultaneous fit of the four $Z \rightarrow \tau\tau$ decay channels with final states $\mu\mu, e\mu, \mu\tau_h$, and $e\tau_h$. As a result of the fit, the combined cross section and τ_h efficiency are measured. The data-to-MC correction factor for the HPS “loose” working point is measured to be 0.94 ± 0.09 . The second approach is based on a comparison of the τ_h channels, $Z \rightarrow \mu\tau_h$ and $e\tau_h$, to the combined $Z \rightarrow \mu\mu, ee$ cross section as measured by CMS. The data-to-MC correction factor for the HPS “loose” working point in this case is measured to be 0.96 ± 0.07 . The slightly smaller uncertainty of the latter method is explained by the higher precision of the combined $Z \rightarrow \mu\mu, ee$ cross-section measurement. These values are also presented in table 2. Both approaches yield more precise uncertainties, 9% and 7%, than the 24% from the tag-and-probe method, for the “loose” HPS working point. To achieve this precision, the methods rely on assumptions about the physics source of the signal, i.e., the values of the inclusive Z production cross section and $Z \rightarrow \tau\tau$ branching fraction, and the absence of non-SM sources in the data sample. In physics analyses where these assumptions cannot be made, such as the measurement of the $Z \rightarrow \tau\tau$ production cross section itself [5] and the search for $H \rightarrow \tau\tau$ [6], the tag-and-probe method remains the only one available.

The expected τ_h efficiency values from the $Z \rightarrow \tau\tau$ process, with a reconstructed $|\eta_{\tau_h}| < 2.3$, and either $p_T^{\tau_h} > 15 \text{ GeV}/c$ or $p_T^{\tau_h} > 20 \text{ GeV}/c$, are estimated using simulated events and presented in table 3. The selections are applied both at the generated and reconstructed levels. A matching of $\Delta R < 0.15$ between the generated and reconstructed τ_h directions is required. Figure 2 shows the expected efficiencies as a function of the generated $p_T^{\tau_h}$ for all working points of each algorithm.

5 Reconstruction of the τ_h decay mode

The correlation between the generated and reconstructed τ_h decay modes is studied using a sample of simulated $Z \rightarrow \tau\tau$ events. The results are presented in figure 3 (left). Each column represents one generated decay mode normalized to unity. Each row corresponds to one reconstructed decay

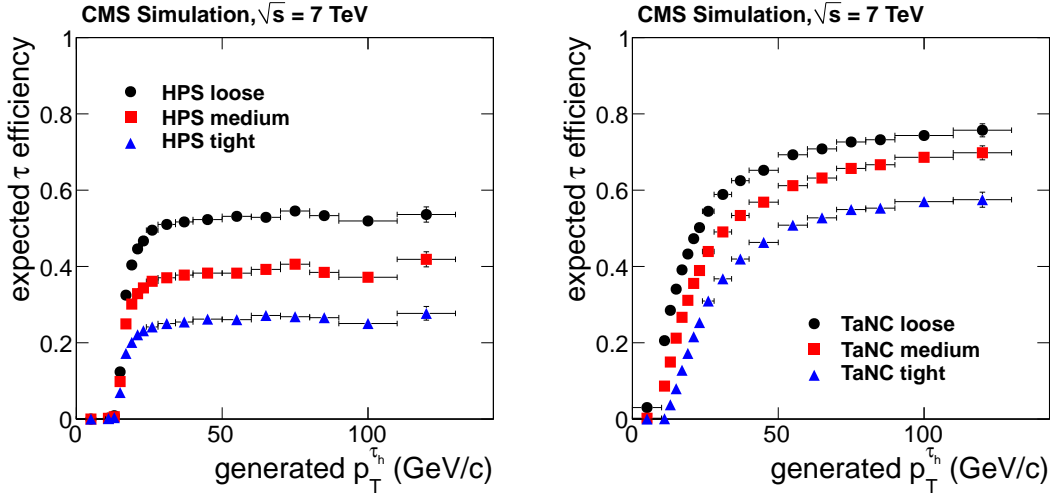


Figure 2. The expected efficiency of the τ_h algorithms as a function of generated $p_T^{\tau_h}$, estimated using a sample of simulated $Z \rightarrow \tau\tau$ events for the HPS (left) and TaNC (right) algorithms, for the “loose”, “medium”, and “tight” working points.

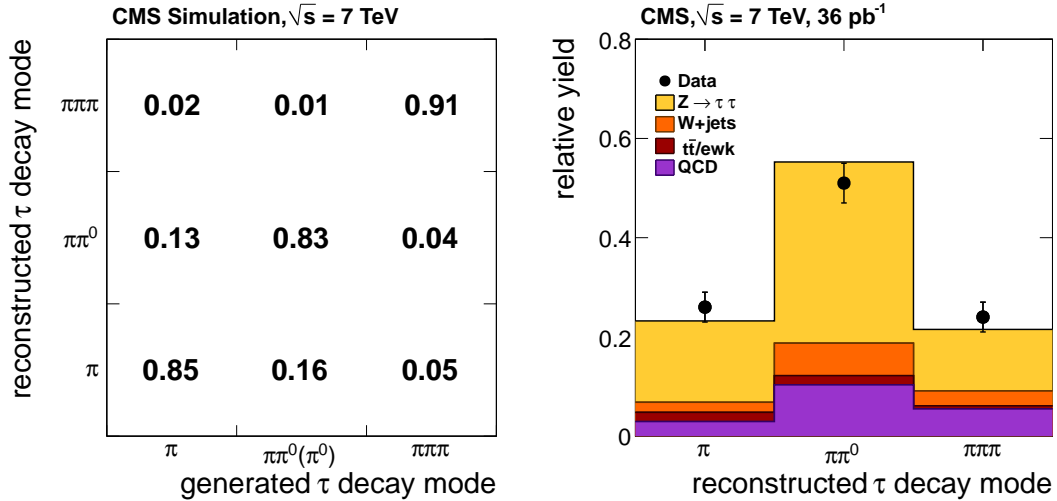


Figure 3. (left) The fraction of generated τ_h decays of a given type reconstructed in a certain decay mode for the HPS “loose” working point from simulated $Z \rightarrow \tau\tau$ events. (right) The relative yield of τ_h reconstructed in different decay modes in the $Z \rightarrow \tau\tau \rightarrow \mu\tau_h$ data sample compared to the MC predictions. The MC simulation is a mixture of the signal and background samples based on the corresponding cross sections, as shown by the histograms.

mode. The numbers demonstrate the fraction of generated τ_h of a given type reconstructed in a specific decay mode. Both generated and reconstructed τ_h are required to have a visible transverse momentum $p_T^{\tau_h} > 15 \text{ GeV}/c$, and to match within a cone of $\Delta R = 0.15$. For each of the generated decay modes, the fraction of correctly reconstructed decays is more than 80%, reaching 90% for the three-charged-pion decay mode.

A data-to-MC comparison of the relative yield of events reconstructed in different τ_h decay modes in a data sample of $Z \rightarrow \tau\tau \rightarrow \mu\tau_h$ events is shown in figure 3 (right). The events are selected using the requirements described in [5]. The τ_h candidates are required to have visible transverse momenta $p_T^{\tau_h} > 20 \text{ GeV}/c$ within the geometric acceptance $|\eta| < 2.3$. The MC sample represents a mixture of the signal and background MC samples based on the corresponding cross sections. The performance of the τ_h algorithm is well reproduced by the MC simulation.

6 Reconstruction of the τ_h energy

Since charged hadrons and photons are reconstructed with high precision using the PF techniques, the reconstructed τ_h energy is expected to be close to the true energy of its visible decay products. According to simulation, the ratio of the reconstructed to the true visible τ_h energy for the HPS algorithm is constant as a function of energy and within 2% of unity, while for TaNC it decreases by about 2% as $p_T^{\tau_h}$ approaches $60 \text{ GeV}/c$. The η dependence is more pronounced. For both algorithms the reconstructed τ_h energy is underestimated by 5% with respect to the true energy as one moves towards higher η (from barrel to endcap region).

The quality of the τ_h energy scale simulation can be examined by analyzing the $Z \rightarrow \tau\tau \rightarrow \mu\tau_h$ data sample. The reconstructed invariant mass of the $\mu\tau_h$ system is very sensitive to the energy scale of the τ_h , since the muon four-momenta are measured with high precision. By varying the τ_h energy scale simultaneously in the signal and background MC samples, a set of templates is produced. The resulting templates are fitted to the data and the best agreement is achieved by scaling the τ_h energy in simulation by a factor 0.97 ± 0.03 , where the uncertainty is averaged over the pseudorapidity range of the data sample. Details of the template fit method and $\mu\tau_h$ invariant mass distributions can be found in [5].

A complementary procedure, which does not assume knowledge of the $\tau\tau$ invariant mass spectrum, is based on the invariant mass of reconstructed τ_h constituents, shown in figure 4. The method uses τ_h as an independent object but relies on good understanding of underlying background events that contribute to the signal sample. The fit is performed separately for $\pi\pi^0$ and $\pi\pi\pi$ decay channels, since the major source of the uncertainty is expected to come from reconstruction of the electromagnetic energy. The simulation describes both decay channels well. The best agreement is achieved by scaling the τ_h energy in simulation by a factor 0.97 ± 0.03 for the $\pi\pi^0$ decay mode and by a factor 1.01 ± 0.02 for the $\pi\pi\pi$ decay mode, where the uncertainties represent full, statistical and systematic, uncertainties of the fit. The effect of the energy-scale uncertainty on the shape of the τ_h invariant mass distribution is also shown in figure 4. Varying the energy scale in simulation by the uncertainty derived from the $\mu\tau_h$ invariant mass fit, i.e. 3%, corresponds to a significant deviation in the predicted τ_h mass shape.

7 Measurement of the τ_h misidentification rate for jets

Jets that could be misidentified as τ_h have different properties depending on their origin. Most of the jets are produced in QCD processes, either with or without the associated production of Z or W bosons. To distinguish between them, different data samples are selected. The QCD-type, gluon-enriched, jets are selected using events with at least one jet of transverse momentum

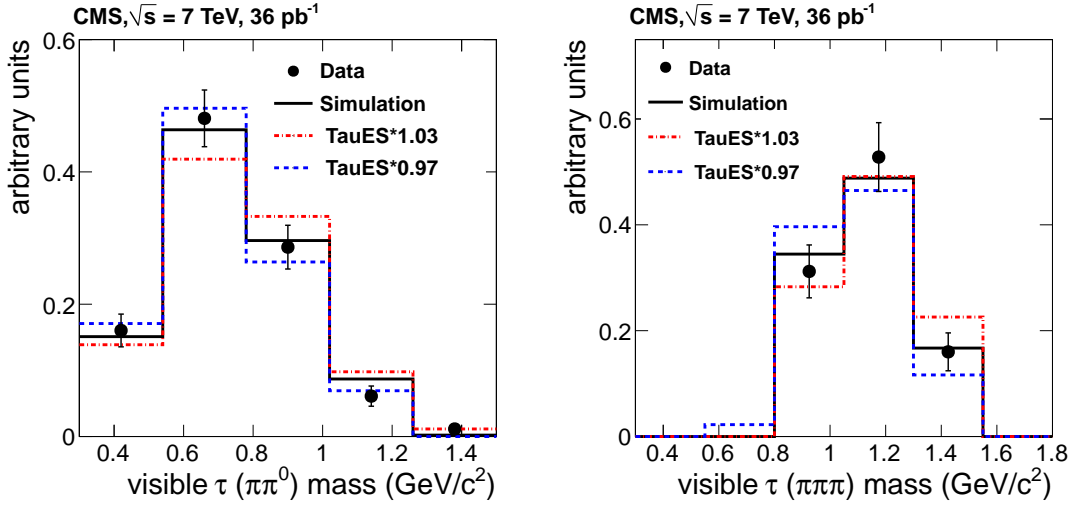


Figure 4. The reconstructed invariant mass of τ_h decaying into one charged and one neutral pion (left) and into three charged pions (right) from data, compared to predictions of the simulation. The solid lines represent results of the best fit described in the text and the dashed lines represent the predictions with the tau energy scale, TauES, varied up and down by 3% with respect to the best fit value.

$p_T^{\text{jet}} > 15 \text{ GeV}/c$ and a second jet of $p_T^{\text{jet}} > 10 \text{ GeV}/c$, both within $|\eta| < 2.5$. The Z- and W-type, quark-enriched, jets are selected by requiring at least one isolated muon with transverse momentum $p_T > 15 \text{ GeV}/c$ and $|\eta| < 2.1$ and a jet of transverse momentum $p_T^{\text{jet}} > 10 \text{ GeV}/c$ within $|\eta| < 2.5$. In addition, a muon-enriched QCD sample is selected by requiring a muon and a jet, but suppressing the W contribution by selecting events with $M_T < 40 \text{ GeV}/c^2$. For each of these samples additional selection requirements are applied to suppress the background contribution from events with jets from other sources.

Figure 5 shows the τ_h misidentification rate as a function of the jet p_T for the “loose” working points of the HPS and TaNC algorithms, where the measured values are compared with the MC predictions for the different types of jets. The misidentification rates expected from simulation, and the measured data-to-MC ratios are summarized in table 4 for the three working points of both reconstruction algorithms. The values are integrated over the p_T and η phase space used in the $Z \rightarrow \tau\tau$ analysis, $p_T^{\text{jet}} > 20 \text{ GeV}/c$ and $|\eta| < 2.3$. The misidentification rate as a function of reconstruction efficiency for all working points of both algorithms is shown in figure 6, which summarizes the MC estimated efficiency and the measured misidentification rate values presented in tables 3 and 4. Since the QCD and μ -enriched QCD misidentification rate values are observed to be similar, only one set of QCD points is shown. Open symbols represent results obtained by running an early fixed-cone τ_h -identification algorithm, used in the CMS physics technical design report (PTDR, [18]) on simulated events. The decay-mode-based HPS and TaNC algorithms perform significantly better than the fixed-cone algorithm.

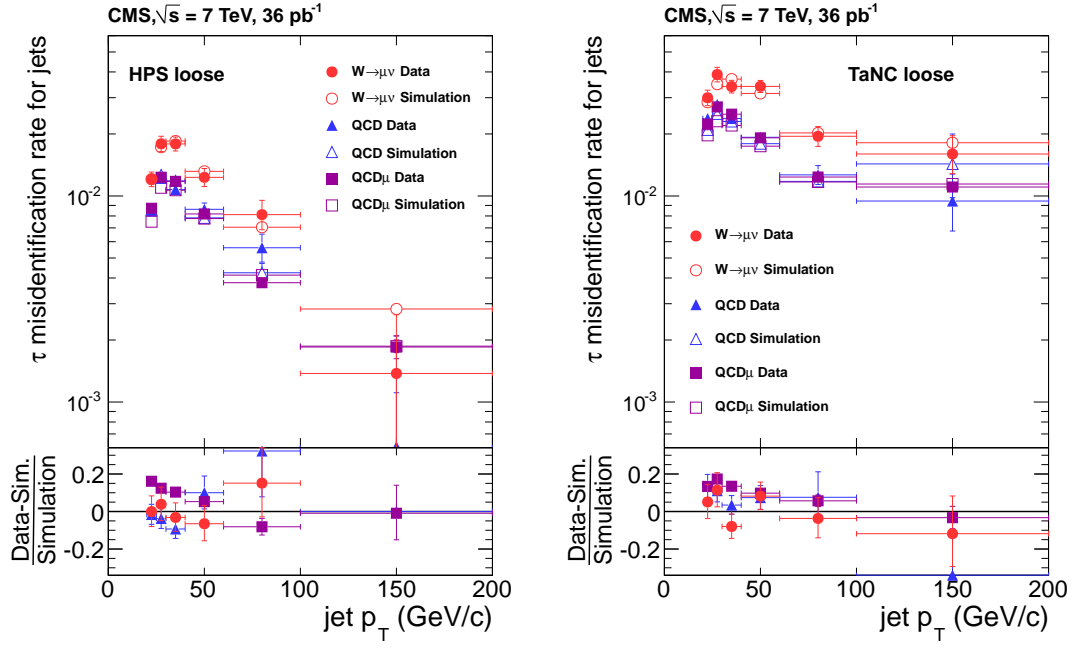


Figure 5. Misidentification probabilities for jets to pass “loose” working points of the HPS (left) and TaNC (right) algorithms as a function of jet p_T for QCD, μ -enriched QCD, and W type events. The misidentification rates measured in data are shown by solid symbols and compared to MC prediction, displayed with open symbols.

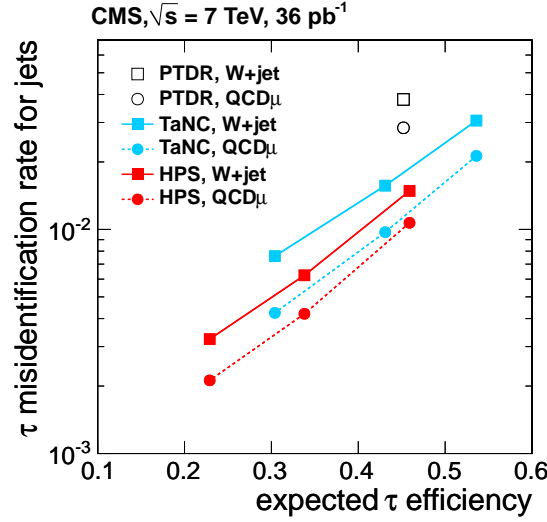


Figure 6. The measured τ_h misidentification rate as a function of the MC-estimated τ_h reconstruction efficiency for the three working points of the HPS and TaNC algorithms from μ -enriched QCD and W data samples. For each algorithm the “loose”, “medium”, and “tight” selections are the points with highest, middle and lowest efficiencies respectively. The PTDR points represent results of the fixed-cone τ_h -identification algorithm [18] on simulation.

Table 4. The MC predicted τ_h misidentification rates and the measured data-to-MC ratios, integrated over the p_T and η phase space typical for the $Z \rightarrow \tau\tau$ analysis.

Algorithm	QCD		QCD μ		W + jets	
	MC (%)	Data/MC	MC (%)	Data/MC	MC (%)	Data/MC
HPS “loose”	1.0	1.00 ± 0.04	1.0	1.07 ± 0.01	1.5	0.99 ± 0.04
HPS “medium”	0.4	1.02 ± 0.06	0.4	1.05 ± 0.02	0.6	1.04 ± 0.06
HPS “tight”	0.2	0.94 ± 0.09	0.2	1.06 ± 0.02	0.3	1.08 ± 0.09
TaNC “loose”	2.1	1.05 ± 0.04	1.9	1.12 ± 0.01	3.0	1.02 ± 0.05
TaNC “medium”	1.3	1.05 ± 0.05	0.9	1.08 ± 0.02	1.6	0.98 ± 0.07
TaNC “tight”	0.5	0.98 ± 0.07	0.4	1.06 ± 0.02	0.8	0.95 ± 0.09

8 Measurement of the τ_h misidentification rate for electrons

Isolated electrons passing the identification and isolation criteria of the τ_h algorithms are also an important source of background in many analyses with τ_h in the final state. In this case the electron is misidentified as a pion originating from τ_h . A multivariate discriminant is used to reduce this background. The discriminant is implemented as a boosted decision tree [19] in the PF algorithm and trained to optimally separate genuine electrons in jets from pions. It uses a set of 14 variables. Two of them contain purely calorimetric information: the fraction of calorimetric energy measured by HCAL and the second moment of the ECAL energy deposit along the η direction. The remaining 12 variables combine calorimetric and tracking information to assess the compatibility of the calorimeter energy deposit with the signature measured in the tracking system. The output of the discriminant is denoted by ξ . The value of the discriminant ξ ranges between -1.0 (most compatible with the pion hypothesis) and 1.0 (most compatible with the electron hypothesis).

Two selected working points, corresponding to $\xi < -0.1$ and $\xi < 0.6$, are considered in this analysis. The first working point rejects even those electrons, that are poorly reconstructed and is optimized for a low misidentification rate, about 2%, at the price of about 4% losses of genuine τ_h . The second working point suffers from larger misidentification rates of about 20%, since it was optimized for τ_h efficiencies exceeding 99.5%. It rejects only well identified electrons.

The probability for an electron to be misidentified as τ_h , the $e \rightarrow \tau_h$ misidentification rate, is determined using a sample of isolated electrons coming from the decay $Z \rightarrow ee$. The events are required to have a reconstructed electron and an electron that is reconstructed as τ_h . The particles must have opposite charge. The invariant mass of the pair is required to be between 60 and 120 GeV/c^2 . The tag electron is required to be isolated and to have a p_T in excess of 25 GeV/c . The second electron, a probe, is required to pass the HPS “loose” working point, without requiring any specific veto against electrons, and have p_T in excess of 15 GeV/c . The $e \rightarrow \tau_h$ misidentification rate is estimated by measuring the ratio between the number of probes passing the electron-rejection discriminant and the overall number of selected probes. The sample of events that does not pass the electron-rejection discriminant, is populated by well-reconstructed electrons. The sample that passes the discriminant contains poorly reconstructed electrons, as well as other background contributions, “misidentified electrons”. To remove the contamination from misidentified electrons, a background subtraction procedure is performed by fitting the passing and failing $e\tau_h$ invariant mass distributions to the superposition of signal and background components.

Table 5. The $e \rightarrow \tau_h$ misidentification rates, found by applying the tag-and-probe method to the MC simulation and the ratio of the tag-and-probe values obtained in data and MC simulation, shown in two regions of η and for two working points of the electron-rejection discriminant. The uncertainties represent the full uncertainties of the method calculated by adding the statistical and systematic uncertainties in quadrature.

Bin	Discriminant $\xi < -0.1$		Discriminant $\xi < 0.6$	
	MC (%)	Data/MC	MC (%)	Data/MC
$ \eta < 1.5$	2.21 ± 0.05	1.13 ± 0.17	13.10 ± 0.08	1.14 ± 0.04
$ \eta > 1.5$	3.96 ± 0.09	0.82 ± 0.18	26.80 ± 0.16	0.90 ± 0.04

Table 5 gives the ratio between the misidentification rates as measured in the data and those obtained using MC simulation for two $|\eta|$ bins. In the central η region, the simulation underestimates the measured misidentification rates. Within the uncertainties of the measurement the data-to-MC ratios for both discriminants agree in the same η intervals.

9 Summary

The performances of two reconstruction algorithms for hadronic tau decays developed by CMS, HPS and TaNC, have been studied using the data sample collected at a centre-of-mass energy of 7 TeV in 2010 and corresponding to an integrated luminosity of 36 pb^{-1} . Both algorithms show good performance in terms of τ_h identification efficiency, approximately 50%, while keeping the misidentification rate for jets at the level of $\sim 1\%$. The MC simulation was found to describe the data well. The τ_h identification efficiency was measured with an uncertainty of 24% by using a tag-and-probe method in a $Z \rightarrow \tau\tau \rightarrow \mu\tau_h$ data sample, and with an uncertainty of 7% by using a global fit to all $Z \rightarrow \tau\tau$ decay channels and constraining the yield to the measured combined $Z \rightarrow \mu\mu, ee$ cross section. The scale factor for measured τ_h energies was found to be close to unity with a relative uncertainty less than 3%.

Acknowledgments

We wish to congratulate our colleagues in the CERN accelerator departments for the excellent performance of the LHC machine. We thank the technical and administrative staff at CERN and other CMS institutes. This work was supported by the Austrian Federal Ministry of Science and Research; the Belgium Fonds de la Recherche Scientifique, and Fonds voor Wetenschappelijk Onderzoek; the Brazilian Funding Agencies (CNPq, CAPES, FAPERJ, and FAPESP); the Bulgarian Ministry of Education and Science; CERN; the Chinese Academy of Sciences, Ministry of Science and Technology, and National Natural Science Foundation of China; the Colombian Funding Agency (COLCIENCIAS); the Croatian Ministry of Science, Education and Sport; the Research Promotion Foundation, Cyprus; the Estonian Academy of Sciences and NICPB; the Academy of Finland, Finnish Ministry of Education and Culture, and Helsinki Institute of Physics; the Institut National de Physique Nucléaire et de Physique des Particules / CNRS, and Commissariat à l'Énergie Atomique et aux Énergies Alternatives / CEA, France; the Bundesministerium für Bildung und Forschung, Deutsche Forschungsgemeinschaft, and Helmholtz-Gemeinschaft Deutscher

Forschungszentren, Germany; the General Secretariat for Research and Technology, Greece; the National Scientific Research Foundation, and National Office for Research and Technology, Hungary; the Department of Atomic Energy and the Department of Science and Technology, India; the Institute for Studies in Theoretical Physics and Mathematics, Iran; the Science Foundation, Ireland; the Istituto Nazionale di Fisica Nucleare, Italy; the Korean Ministry of Education, Science and Technology and the World Class University program of NRF, Korea; the Lithuanian Academy of Sciences; the Mexican Funding Agencies (CINVESTAV, CONACYT, SEP, and UASLP-FAI); the Ministry of Science and Innovation, New Zealand; the Pakistan Atomic Energy Commission; the State Commission for Scientific Research, Poland; the Fundação para a Ciência e a Tecnologia, Portugal; JINR (Armenia, Belarus, Georgia, Ukraine, Uzbekistan); the Ministry of Science and Technologies of the Russian Federation, the Russian Ministry of Atomic Energy and the Russian Foundation for Basic Research; the Ministry of Science and Technological Development of Serbia; the Ministerio de Ciencia e Innovación, and Programa Consolider-Ingenio 2010, Spain; the Swiss Funding Agencies (ETH Board, ETH Zurich, PSI, SNF, UniZH, Canton Zurich, and SER); the National Science Council, Taipei; the Scientific and Technical Research Council of Turkey, and Turkish Atomic Energy Authority; the Science and Technology Facilities Council, U.K.; the US Department of Energy, and the US National Science Foundation.

Individuals have received support from the Marie-Curie programme and the European Research Council (European Union); the Leventis Foundation; the A. P. Sloan Foundation; the Alexander von Humboldt Foundation; the Belgian Federal Science Policy Office; the Fonds pour la Formation à la Recherche dans l'Industrie et dans l'Agriculture (FRIA-Belgium); the Agentschap voor Innovatie door Wetenschap en Technologie (IWT-Belgium); and the Council of Science and Industrial Research, India.

References

- [1] CMS collaboration, *The CMS experiment at the CERN LHC*, [*JINST* **03** \(2008\) S08004](#).
- [2] L. Evans and P. Bryant, *LHC Machine*, [*JINST* **03** \(2008\) S08001](#).
- [3] S. P. Martin, *A supersymmetry primer*, 1997, see also references therein.
- [4] B. Dutta and R.N. Mohapatra, *Phenomenology of light remnant doubly charged Higgs fields in the supersymmetric left-right model*, [*Phys. Rev. D* **59** \(1999\) 015018](#) [[hep-ph/9804277](#)].
- [5] CMS collaboration, *Measurement of the Inclusive Z Cross Section via Decays to Tau Pairs in pp Collisions at $\sqrt{s} = 7$ TeV*, [*JHEP* **08** \(2011\) 117](#) [[arXiv:1104.1617v1](#)].
- [6] CMS collaboration, *Search for Neutral MSSM Higgs Bosons Decaying to Tau Pairs in pp Collisions at $\sqrt{s} = 7$ TeV*, [*Phys. Rev. Lett.* **106** \(2011\) 231801](#).
- [7] CMS collaboration, *CMS tracking performance results from early LHC operation*, [*Eur. Phys. J. C* **70** \(2010\) 1165](#).
- [8] CMS collaboration, *Particle–Flow Event Reconstruction in CMS and Performance for Jets, Taus and E_T^{miss}* , CMS Physics Analysis Summary CMS-PAS-PFT-09-001, 2009.
- [9] PARTICLE DATA GROUP collaboration, K. Nakamura et al., *Review of particle physics*, [*J. Phys. G* **37** \(2010\) 075021](#).

- [10] M. Cacciari, G. P. Salam and G. Soyez, *The anti- k_t jet clustering algorithm*, *JHEP* **04** (2008) 063 [[arXiv:0802.1189](#)].
- [11] S. Alioli, P. Nason, C. Oleari and E. Re, *NLO vector-boson production matched with shower in POWHEG*, *JHEP* **07** (2008) 060 [[arXiv:0805.4802](#)].
- [12] P. Nason, *A new method for combining NLO QCD with shower Monte Carlo algorithms*, *JHEP* **11** (2004) 040 [[hep-ph/0409146](#)].
- [13] S. Frixione, P. Nason and C. Oleari, *Matching NLO QCD computations with Parton Shower simulations: the POWHEG method*, *JHEP* **11** (2007) 070 [[arXiv:0709.2092](#)].
- [14] T. Sjöstrand, S. Mrenna and P.Z. Skands, *PYTHIA 6.4 Physics and Manual*, *JHEP* **05** (2006) 026 [[hep-ph/0603175](#)].
- [15] F. Maltoni and T. Stelzer, *MadEvent: Automatic event generation with MadGraph*, *JHEP* **02** (2003) 027 [[hep-ph/0208156](#)].
- [16] S. Jadach, Z. Wąs, R. Decker and J.H. Kuhn, *The tau decay library TAUOLA: Version 2.4*, *Comput. Phys. Commun.* **76** (1993) 361.
- [17] CMS collaboration, *CMS High Level Trigger*, LHCC Report CERN-LHCC-2007-021, 2007.
- [18] CMS collaboration, *CMS technical design report, volume II: Physics performance*, *J. Phys. G* **34** (2007) 995.
- [19] B.P. Roe, H.-J. Yang, J. Zhu, Y. Liu, I. Stancu and G. McGregor, *Boosted Decision Trees as an Alternative to Artificial Neural Networks for Particle Identification*, *Nucl. Instrum. Meth A* **543** (2005) 577 [[physics/0408124v2](#)].

The CMS collaboration

Yerevan Physics Institute, Yerevan, Armenia

S. Chatrchyan, V. Khachatryan, A.M. Sirunyan, A. Tumasyan

Institut für Hochenergiephysik der OeAW, Wien, Austria

W. Adam, T. Bergauer, M. Dragicevic, J. Erö, C. Fabjan, M. Friedl, R. Frühwirth, V.M. Ghete, J. Hammer¹, S. Häseler, M. Hoch, N. Hörmann, J. Hrubec, M. Jeitler, W. Kiesenhofer, M. Krammer, D. Liko, I. Mikulec, M. Pernicka, B. Rahbaran, H. Rohringer, R. Schöfbeck, J. Strauss, A. Taurok, F. Teischinger, C. Trauner, P. Wagner, W. Waltenberger, G. Walzel, E. Widl, C.-E. Wulz

National Centre for Particle and High Energy Physics, Minsk, Belarus

V. Mossolov, N. Shumeiko, J. Suarez Gonzalez

Universiteit Antwerpen, Antwerpen, Belgium

S. Bansal, L. Benucci, E.A. De Wolf, X. Janssen, S. Luyckx, T. Maes, L. Mucibello, S. Ochesanu, B. Roland, R. Rougny, M. Selvaggi, H. Van Haevermaet, P. Van Mechelen, N. Van Remortel

Vrije Universiteit Brussel, Brussel, Belgium

F. Blekman, S. Blyweert, J. D'Hondt, R. Gonzalez Suarez, A. Kalogeropoulos, M. Maes, A. Olbrechts, W. Van Doninck, P. Van Mulders, G.P. Van Onsem, I. Villella

Université Libre de Bruxelles, Bruxelles, Belgium

O. Charaf, B. Clerbaux, G. De Lentdecker, V. Dero, A.P.R. Gay, G.H. Hammad, T. Hreus, P.E. Marage, A. Raval, L. Thomas, G. Vander Marcken, C. Vander Velde, P. Vanlaer

Ghent University, Ghent, Belgium

V. Adler, A. Cimmino, S. Costantini, M. Grunewald, B. Klein, J. Lellouch, A. Marinov, J. McCartin, D. Ryckbosch, F. Thyssen, M. Tytgat, L. Vanelderen, P. Verwilligen, S. Walsh, N. Zaganidis

Université Catholique de Louvain, Louvain-la-Neuve, Belgium

S. Basegmez, G. Bruno, J. Caudron, L. Ceard, E. Cortina Gil, J. De Favereau De Jeneret, C. Delaere, D. Favart, A. Giammanco, G. Grégoire, J. Hollar, V. Lemaitre, J. Liao, O. Militaru, C. Nuttens, S. Oryn, D. Pagano, A. Pin, K. Piotrkowski, N. Schul

Université de Mons, Mons, Belgium

N. Beliy, T. Caebergs, E. Daubie

Centro Brasileiro de Pesquisas Fisicas, Rio de Janeiro, Brazil

G.A. Alves, L. Brito, D. De Jesus Damiao, M.E. Pol, M.H.G. Souza

Universidade do Estado do Rio de Janeiro, Rio de Janeiro, Brazil

W.L. Aldá Júnior, W. Carvalho, E.M. Da Costa, C. De Oliveira Martins, S. Fonseca De Souza, D. Matos Figueiredo, L. Mundim, H. Nogima, V. Oguri, W.L. Prado Da Silva, A. Santoro, S.M. Silva Do Amaral, A. Sznajder

Instituto de Fisica Teorica, Universidade Estadual Paulista, Sao Paulo, Brazil

T.S. Anjos², C.A. Bernardes², F.A. Dias³, T.R. Fernandez Perez Tomei, E. M. Gregores², C. Lagana, F. Marinho, P.G. Mercadante², S.F. Novaes, Sandra S. Padula

Institute for Nuclear Research and Nuclear Energy, Sofia, Bulgaria

N. Darmenov¹, V. Genchev¹, P. Iaydjiev¹, S. Piperov, M. Rodozov, S. Stoykova, G. Sultanov, V. Tcholakov, R. Trayanov, M. Vutova

University of Sofia, Sofia, Bulgaria

A. Dimitrov, R. Hadjiiska, A. Karadzhinova, V. Kozhuharov, L. Litov, M. Mateev, B. Pavlov, P. Petkov

Institute of High Energy Physics, Beijing, China

J.G. Bian, G.M. Chen, H.S. Chen, C.H. Jiang, D. Liang, S. Liang, X. Meng, J. Tao, J. Wang, J. Wang, X. Wang, Z. Wang, H. Xiao, M. Xu, J. Zang, Z. Zhang

State Key Lab. of Nucl. Phys. and Tech., Peking University, Beijing, China

Y. Ban, S. Guo, Y. Guo, W. Li, Y. Mao, S.J. Qian, H. Teng, B. Zhu, W. Zou

Universidad de Los Andes, Bogota, Colombia

A. Cabrera, B. Gomez Moreno, A.A. Ocampo Rios, A.F. Osorio Oliveros, J.C. Sanabria

Technical University of Split, Split, Croatia

N. Godinovic, D. Lelas, K. Lelas, R. Plestina⁴, D. Polic, I. Puljak

University of Split, Split, Croatia

Z. Antunovic, M. Dzelalija, M. Kovac

Institute Rudjer Boskovic, Zagreb, Croatia

V. Brigljevic, S. Duric, K. Kadija, J. Luetic, S. Morovic

University of Cyprus, Nicosia, Cyprus

A. Attikis, M. Galanti, J. Mousa, C. Nicolaou, F. Ptochos, P.A. Razis

Charles University, Prague, Czech Republic

M. Finger, M. Finger Jr.

Academy of Scientific Research and Technology of the Arab Republic of Egypt, Egyptian Network of High Energy Physics, Cairo, Egypt

Y. Assran⁵, A. Ellithi Kamel⁶, S. Khalil⁷, M.A. Mahmoud⁸, A. Radi⁹

National Institute of Chemical Physics and Biophysics, Tallinn, Estonia

A. Hektor, M. Kadastik, M. Müntel, M. Raidal, L. Rebane, A. Tiko

Department of Physics, University of Helsinki, Helsinki, Finland

V. Azzolini, P. Eerola, G. Fedi, M. Voutilainen

Helsinki Institute of Physics, Helsinki, Finland

S. Czellar, J. Härkönen, A. Heikkinen, V. Karimäki, R. Kinnunen, M.J. Kortelainen, T. Lampén, K. Lassila-Perini, S. Lehti, T. Lindén, P. Luukka, T. Mäenpää, E. Tuominen, J. Tuominiemi, E. Tuovinen, D. Ungaro, L. Wendland

Lappeenranta University of Technology, Lappeenranta, Finland

K. Banzuzi, A. Karjalainen, A. Korpela, T. Tuuva

Laboratoire d'Annecy-le-Vieux de Physique des Particules, IN2P3-CNRS, Annecy-le-Vieux, France

D. Sillou

DSM/IRFU, CEA/Saclay, Gif-sur-Yvette, France

M. Besancon, S. Choudhury, M. Dejardin, D. Denegri, B. Fabbro, J.L. Faure, F. Ferri, S. Ganjour, A. Givernaud, P. Gras, G. Hamel de Monchenault, P. Jarry, E. Locci, J. Malcles, M. Marionneau, L. Millischer, J. Rander, A. Rosowsky, I. Shreyber, M. Titov

Laboratoire Leprince-Ringuet, Ecole Polytechnique, IN2P3-CNRS, Palaiseau, France

S. Baffioni, F. Beaudette, L. Benhabib, L. Bianchini, M. Bluj¹⁰, C. Broutin, P. Busson, C. Charlot, T. Dahms, L. Dobrzynski, S. Elgammal, R. Granier de Cassagnac, M. Haguenauer, P. Miné, C. Mironov, C. Ochando, P. Paganini, D. Sabes, R. Salerno, Y. Sirois, C. Thiebaux, C. Veelken, A. Zabi

Institut Pluridisciplinaire Hubert Curien, Université de Strasbourg, Université de Haute Alsace Mulhouse, CNRS/IN2P3, Strasbourg, France

J.-L. Agram¹¹, J. Andrea, D. Bloch, D. Bodin, J.-M. Brom, M. Cardaci, E.C. Chabert, C. Collard, E. Conte¹¹, F. Drouhin¹¹, C. Ferro, J.-C. Fontaine¹¹, D. Gelé, U. Goerlach, S. Greder, P. Juillot, M. Karim¹¹, A.-C. Le Bihan, Y. Mikami, P. Van Hove

Centre de Calcul de l'Institut National de Physique Nucleaire et de Physique des Particules (IN2P3), Villeurbanne, France

F. Fassi, D. Mercier

Université de Lyon, Université Claude Bernard Lyon 1, CNRS-IN2P3, Institut de Physique Nucléaire de Lyon, Villeurbanne, France

C. Baty, S. Beauceron, N. Beaupere, M. Bedjidian, O. Bondu, G. Boudoul, D. Boumediene, H. Brun, J. Chasserat, R. Chierici, D. Contardo, P. Depasse, H. El Mamouni, J. Fay, S. Gascon, B. Ille, T. Kurca, T. Le Grand, M. Lethuillier, L. Mirabito, S. Perries, V. Sordini, S. Tosi, Y. Tschudi, P. Verdier, S. Viret

Institute of High Energy Physics and Informatization, Tbilisi State University, Tbilisi, Georgia

D. Lomidze

RWTH Aachen University, I. Physikalisches Institut, Aachen, Germany

G. Anagnostou, S. Beranek, M. Edelhoff, L. Feld, N. Heracleous, O. Hindrichs, R. Jussen, K. Klein, J. Merz, N. Mohr, A. Ostapchuk, A. Perieanu, F. Raupach, J. Sammet, S. Schael, D. Sprenger, H. Weber, M. Weber, B. Wittmer, V. Zhukov¹²

RWTH Aachen University, III. Physikalisches Institut A, Aachen, Germany

M. Ata, E. Dietz-Laursonn, M. Erdmann, T. Hebbeker, C. Heidemann, A. Hinzmann, K. Hoepfner, T. Klimkovich, D. Klingebiel, P. Kreuzer, D. Lanske[†], J. Lingemann, C. Magass, M. Merschmeyer, A. Meyer, P. Papacz, H. Pieta, H. Reithler, S.A. Schmitz, L. Sonnenschein, J. Steggemann, D. Teyssier

RWTH Aachen University, III. Physikalisches Institut B, Aachen, Germany

M. Bontenackels, V. Cherepanov, M. Davids, G. Flügge, H. Geenen, M. Giffels, W. Haj Ahmad, F. Hoehle, B. Kargoll, T. Kress, Y. Kuessel, A. Linn, A. Nowack, L. Perchalla, O. Pooth, J. Rennefeld, P. Sauerland, A. Stahl, D. Tornier, M.H. Zoeller

Deutsches Elektronen-Synchrotron, Hamburg, Germany

M. Aldaya Martin, W. Behrenhoff, U. Behrens, M. Bergholz¹³, A. Bethani, K. Borras, A. Cakir, A. Campbell, E. Castro, D. Dammann, G. Eckerlin, D. Eckstein, A. Flossdorf, G. Flucke, A. Geiser, J. Hauk, H. Jung¹, M. Kasemann, P. Katsas, C. Kleinwort, H. Kluge, A. Knutsson, M. Krämer, D. Krücker, E. Kuznetsova, W. Lange, W. Lohmann¹³, B. Lutz, R. Mankel, M. Marienfeld, I.-A. Melzer-Pellmann, A.B. Meyer, J. Mnich, A. Mussgiller, J. Olzem, A. Petrukhin, D. Pitzl, A. Raspereza, M. Rosin, R. Schmidt¹³, T. Schoerner-Sadenius, N. Sen, A. Spiridonov, M. Stein, J. Tomaszewska, R. Walsh, C. Wissing

University of Hamburg, Hamburg, Germany

C. Autermann, V. Blobel, S. Bobrovskiy, J. Draeger, H. Enderle, U. Gebbert, M. Görner, T. Hermanns, K. Kaschube, G. Kaussen, H. Kirschenmann, R. Klanner, J. Lange, B. Mura, S. Naumann-Emme, F. Nowak, N. Pietsch, C. Sander, H. Schettler, P. Schleper, E. Schlieckau, M. Schröder, T. Schum, H. Stadie, G. Steinbrück, J. Thomsen

Institut für Experimentelle Kernphysik, Karlsruhe, Germany

C. Barth, J. Bauer, J. Berger, V. Buege, T. Chwalek, W. De Boer, A. Dierlamm, G. Dirkes, M. Feindt, J. Gruschke, C. Hackstein, F. Hartmann, M. Heinrich, H. Held, K.H. Hoffmann, S. Hone, I. Katkov¹², J.R. Komaragiri, T. Kuhr, D. Martschei, S. Mueller, Th. Müller, M. Niegel, O. Oberst, A. Oehler, J. Ott, T. Peiffer, G. Quast, K. Rabbertz, F. Ratnikov, N. Ratnikova, M. Renz, S. Röcker, C. Saout, A. Scheurer, P. Schieferdecker, F.-P. Schilling, M. Schmanau, G. Schott, H.J. Simonis, F.M. Stober, D. Troendle, J. Wagner-Kuhr, T. Weiler, M. Zeise, E.B. Ziebarth

Institute of Nuclear Physics "Demokritos", Aghia Paraskevi, Greece

G. Daskalakis, T. Geralis, S. Kesisoglou, A. Kyriakis, D. Loukas, I. Manolakos, A. Markou, C. Markou, C. Mavrommatis, E. Ntomari, E. Petrakou

University of Athens, Athens, Greece

L. Gouskos, T.J. Mertzimekis, A. Panagiotou, N. Saoulidou, E. Stiliaris

University of Ioánnina, Ioánnina, Greece

I. Evangelou, C. Foudas¹, P. Kokkas, N. Manthos, I. Papadopoulos, V. Patras, F.A. Triantis

KFKI Research Institute for Particle and Nuclear Physics, Budapest, Hungary

A. Aranyi, G. Bencze, L. Boldizsar, C. Hajdu¹, P. Hidas, D. Horvath¹⁴, A. Kapusi, K. Krajczar¹⁵, F. Sikler¹, G.I. Veres¹⁵, G. Vesztegombi¹⁵

Institute of Nuclear Research ATOMKI, Debrecen, Hungary

N. Beni, J. Molnar, J. Palinkas, Z. Szillasi, V. Veszpremi

University of Debrecen, Debrecen, Hungary

J. Karancsi, P. Raics, Z.L. Trocsanyi, B. Ujvari

Panjab University, Chandigarh, India

S.B. Beri, V. Bhatnagar, N. Dhingra, R. Gupta, M. Jindal, M. Kaur, J.M. Kohli, M.Z. Mehta, N. Nishu, L.K. Saini, A. Sharma, A.P. Singh, J. Singh, S.P. Singh

University of Delhi, Delhi, India

S. Ahuja, B.C. Choudhary, P. Gupta, A. Kumar, A. Kumar, S. Malhotra, M. Naimuddin, K. Ranjan, R.K. Shivpuri

Saha Institute of Nuclear Physics, Kolkata, India

S. Banerjee, S. Bhattacharya, S. Dutta, B. Gomber, S. Jain, S. Jain, R. Khurana, S. Sarkar

Bhabha Atomic Research Centre, Mumbai, India

R.K. Choudhury, D. Dutta, S. Kailas, V. Kumar, P. Mehta, A.K. Mohanty¹, L.M. Pant, P. Shukla

Tata Institute of Fundamental Research - EHEP, Mumbai, India

T. Aziz, M. Guchait¹⁶, A. Gurtu, M. Maity¹⁷, D. Majumder, G. Majumder, T. Mathew, K. Mazumdar, G.B. Mohanty, B. Parida, A. Saha, K. Sudhakar, N. Wickramage

Tata Institute of Fundamental Research - HECR, Mumbai, India

S. Banerjee, S. Dugad, N.K. Mondal

Institute for Research and Fundamental Sciences (IPM), Tehran, Iran

H. Arfaei, H. Bakhshiansohi¹⁸, S.M. Etesami¹⁹, A. Fahim¹⁸, M. Hashemi, H. Hesari, A. Jafari¹⁸, M. Khakzad, A. Mohammadi²⁰, M. Mohammadi Najafabadi, S. Paktinat Mehdiabadi, B. Safarzadeh, M. Zeinali¹⁹

INFN Sezione di Bari ^a, Università di Bari ^b, Politecnico di Bari ^c, Bari, Italy

M. Abbrescia^{a,b}, L. Barbone^{a,b}, C. Calabria^{a,b}, A. Colaleo^a, D. Creanza^{a,c}, N. De Filippis^{a,c,1}, M. De Palma^{a,b}, L. Fiore^a, G. Iaselli^{a,c}, L. Lusito^{a,b}, G. Maggi^{a,c}, M. Maggi^a, N. Manna^{a,b}, B. Marangelli^{a,b}, S. My^{a,c}, S. Nuzzo^{a,b}, N. Pacifico^{a,b}, G.A. Pierro^a, A. Pompili^{a,b}, G. Pugliese^{a,c}, F. Romano^{a,c}, G. Roselli^{a,b}, G. Selvaggi^{a,b}, L. Silvestris^a, R. Trentadue^a, S. Tuppiti^{a,b}, G. Zito^a

INFN Sezione di Bologna ^a, Università di Bologna ^b, Bologna, Italy

G. Abbiendi^a, A.C. Benvenuti^a, D. Bonacorsi^a, S. Braibant-Giacomelli^{a,b}, L. Brigliadori^a, P. Capiluppi^{a,b}, A. Castro^{a,b}, F.R. Cavallo^a, M. Cuffiani^{a,b}, G.M. Dallavalle^a, F. Fabbri^a, A. Fanfani^{a,b}, D. Fasanella^{a,1}, P. Giacomelli^a, M. Giunta^a, C. Grandi^a, S. Marcellini^a, G. Masetti^b, M. Meneghelli^{a,b}, A. Montanari^a, F.L. Navarria^{a,b}, F. Odorici^a, A. Perrotta^a, F. Primavera^a, A.M. Rossi^{a,b}, T. Rovelli^{a,b}, G. Siroli^{a,b}, R. Travaglini^{a,b}

INFN Sezione di Catania ^a, Università di Catania ^b, Catania, Italy

S. Albergo^{a,b}, G. Cappello^{a,b}, M. Chiorboli^{a,b}, S. Costa^{a,b}, R. Potenza^{a,b}, A. Tricomi^{a,b}, C. Tuve^{a,b}

INFN Sezione di Firenze ^a, Università di Firenze ^b, Firenze, Italy

G. Barbagli^a, V. Ciulli^{a,b}, C. Civinini^a, R. D'Alessandro^{a,b}, E. Focardi^{a,b}, S. Frosali^{a,b}, E. Gallo^a, S. Gonzi^{a,b}, M. Meschini^a, S. Paoletti^a, G. Sguazzoni^a, A. Tropiano^{a,1}

INFN Laboratori Nazionali di Frascati, Frascati, Italy

L. Benussi, S. Bianco, S. Colafranceschi²¹, F. Fabbri, D. Piccolo

INFN Sezione di Genova, Genova, Italy

P. Fabbricatore, R. Musenich

INFN Sezione di Milano-Bicocca ^a, Università di Milano-Bicocca ^b, Milano, ItalyA. Benaglia^{a,b,1}, F. De Guio^{a,b}, L. Di Matteo^{a,b}, S. Gennai¹, A. Ghezzi^{a,b}, S. Malvezzi^a, A. Martelli^{a,b}, A. Massironi^{a,b,1}, D. Menasce^a, L. Moroni^a, M. Paganoni^{a,b}, D. Pedrini^a, S. Ragazzi^{a,b}, N. Redaelli^a, S. Sala^a, T. Tabarelli de Fatis^{a,b}**INFN Sezione di Napoli ^a, Università di Napoli "Federico II" ^b, Napoli, Italy**S. Buontempo^a, C.A. Carrillo Montoya^{a,1}, N. Cavallo^{a,22}, A. De Cosa^{a,b}, F. Fabozzi^{a,22}, A.O.M. Iorio^{a,1}, L. Lista^a, M. Merola^{a,b}, P. Paolucci^a**INFN Sezione di Padova ^a, Università di Padova ^b, Università di Trento (Trento) ^c, Padova, Italy**P. Azzi^a, N. Bacchetta^{a,1}, P. Bellan^{a,b}, D. Bisello^{a,b}, A. Branca^a, R. Carlin^{a,b}, P. Checchia^a, T. Dorigo^a, U. Dosselli^a, F. Fanzago^a, F. Gasparini^{a,b}, U. Gasparini^{a,b}, A. Gozzelino, S. Lacaprara^{a,23}, I. Lazzizzera^{a,c}, M. Margoni^{a,b}, M. Mazzucato^a, A.T. Meneguzzo^{a,b}, M. Nespolo^{a,1}, L. Perrozzi^a, N. Pozzobon^{a,b}, P. Ronchese^{a,b}, F. Simonetto^{a,b}, E. Torassa^a, M. Tosi^{a,b,1}, S. Vanini^{a,b}, P. Zotto^{a,b}, G. Zumerle^{a,b}**INFN Sezione di Pavia ^a, Università di Pavia ^b, Pavia, Italy**P. Baesso^{a,b}, U. Berzano^a, S.P. Ratti^{a,b}, C. Riccardi^{a,b}, P. Torre^{a,b}, P. Vitulo^{a,b}, C. Viviani^{a,b}**INFN Sezione di Perugia ^a, Università di Perugia ^b, Perugia, Italy**M. Biasini^{a,b}, G.M. Bilei^a, B. Caponeri^{a,b}, L. Fanò^{a,b}, P. Lariccia^{a,b}, A. Lucaroni^{a,b,1}, G. Mantovani^{a,b}, M. Menichelli^a, A. Nappi^{a,b}, F. Romeo^{a,b}, A. Santocchia^{a,b}, S. Taroni^{a,b,1}, M. Valdata^{a,b}**INFN Sezione di Pisa ^a, Università di Pisa ^b, Scuola Normale Superiore di Pisa ^c, Pisa, Italy**P. Azzurri^{a,c}, G. Bagliesi^a, J. Bernardini^{a,b}, T. Boccali^a, G. Broccolo^{a,c}, R. Castaldi^a, R.T. D'Agnolo^{a,c}, R. Dell'Orso^a, F. Fiori^{a,b}, L. Foà^{a,c}, A. Giassi^a, A. Kraan^a, F. Ligabue^{a,c}, T. Lomtadze^a, L. Martinì^{a,24}, A. Messineo^{a,b}, F. Palla^a, F. Palmonari, G. Segneri^a, A.T. Serban^a, P. Spagnolo^a, R. Tenchini^a, G. Tonelli^{a,b,1}, A. Venturi^{a,1}, P.G. Verdini^a**INFN Sezione di Roma ^a, Università di Roma "La Sapienza" ^b, Roma, Italy**L. Barone^{a,b}, F. Cavallari^a, D. Del Re^{a,b,1}, E. Di Marco^{a,b}, M. Diemoz^a, D. Franci^{a,b}, M. Grassi^{a,1}, E. Longo^{a,b}, P. Meridiani^a, S. Nourbakhsh^a, G. Organtini^{a,b}, F. Pandolfi^{a,b}, R. Paramatti^a, S. Rahatlou^{a,b}, M. Sigamani^a**INFN Sezione di Torino ^a, Università di Torino ^b, Università del Piemonte Orientale (Novara) ^c, Torino, Italy**N. Amapane^{a,b}, R. Arcidiacono^{a,c}, S. Argiro^{a,b}, M. Arneodo^{a,c}, C. Biino^a, C. Botta^{a,b}, N. Cartiglia^a, R. Castello^{a,b}, M. Costa^{a,b}, N. Demaria^a, A. Graziano^{a,b}, C. Mariotti^a, S. Maselli^a, E. Migliore^{a,b}, V. Monaco^{a,b}, M. Musich^a, M.M. Obertino^{a,c}, N. Pastrone^a, M. Pelliccioni^{a,b}, A. Potenza^{a,b}, A. Romero^{a,b}, M. Ruspà^{a,c}, R. Sacchi^{a,b}, V. Sola^{a,b}, A. Solano^{a,b}, A. Staiano^a, A. Vilela Pereira^a

INFN Sezione di Trieste ^a, Università di Trieste ^b, Trieste, Italy

S. Belforte^a, F. Cossutti^a, G. Della Ricca^{a,b}, B. Gobbo^a, M. Marone^{a,b}, D. Montanino^{a,b}, A. Penzo^a

Kangwon National University, Chunchon, Korea

S.G. Heo, S.K. Nam

Kyungpook National University, Daegu, Korea

S. Chang, J. Chung, D.H. Kim, G.N. Kim, J.E. Kim, D.J. Kong, H. Park, S.R. Ro, D.C. Son, T. Son

Chonnam National University, Institute for Universe and Elementary Particles, Kwangju, Korea

J.Y. Kim, Zero J. Kim, S. Song

Konkuk University, Seoul, Korea

H.Y. Jo

Korea University, Seoul, Korea

S. Choi, D. Gyun, B. Hong, M. Jo, H. Kim, J.H. Kim, T.J. Kim, K.S. Lee, D.H. Moon, S.K. Park, E. Seo, K.S. Sim

University of Seoul, Seoul, Korea

M. Choi, S. Kang, H. Kim, C. Park, I.C. Park, S. Park, G. Ryu

Sungkyunkwan University, Suwon, Korea

Y. Cho, Y. Choi, Y.K. Choi, J. Goh, M.S. Kim, B. Lee, J. Lee, S. Lee, H. Seo, I. Yu

Vilnius University, Vilnius, Lithuania

M.J. Bilinskas, I. Grigelionis, M. Janulis, D. Martisiute, P. Petrov, M. Polujanskas, T. Sabonis

Centro de Investigacion y de Estudios Avanzados del IPN, Mexico City, Mexico

H. Castilla-Valdez, E. De La Cruz-Burelo, I. Heredia-de La Cruz, R. Lopez-Fernandez, R. Magaña Villalba, J. Martínez-Ortega, A. Sánchez-Hernández, L.M. Villasenor-Cendejas

Universidad Iberoamericana, Mexico City, Mexico

S. Carrillo Moreno, F. Vazquez Valencia

Benemerita Universidad Autonoma de Puebla, Puebla, Mexico

H.A. Salazar Ibarquen

Universidad Autónoma de San Luis Potosí, San Luis Potosí, Mexico

E. Casimiro Linares, A. Morelos Pineda, M.A. Reyes-Santos

University of Auckland, Auckland, New Zealand

D. Krofcheck, J. Tam

University of Canterbury, Christchurch, New Zealand

P.H. Butler, R. Doesburg, H. Silverwood

National Centre for Physics, Quaid-I-Azam University, Islamabad, Pakistan

M. Ahmad, I. Ahmed, M.H. Ansari, M.I. Asghar, H.R. Hoorani, S. Khalid, W.A. Khan, T. Khurshid, S. Qazi, M.A. Shah, M. Shoaib

Institute of Experimental Physics, Faculty of Physics, University of Warsaw, Warsaw, Poland

G. Brona, M. Cwiok, W. Dominik, K. Doroba, A. Kalinowski, M. Konecki, J. Krolikowski

Soltan Institute for Nuclear Studies, Warsaw, Poland

T. Frueboes, R. Gokieli, M. Górski, M. Kazana, K. Nawrocki, K. Romanowska-Rybinska, M. Szleper, G. Wrochna, P. Zalewski

Laboratório de Instrumentação e Física Experimental de Partículas, Lisboa, Portugal

N. Almeida, P. Bargassa, A. David, P. Faccioli, P.G. Ferreira Parracho, M. Gallinaro¹, P. Musella, A. Nayak, J. Pela¹, P.Q. Ribeiro, J. Seixas, J. Varela

Joint Institute for Nuclear Research, Dubna, Russia

S. Afanasiev, I. Belotelov, P. Bunin, M. Gavrilenko, I. Golutvin, A. Kamenev, V. Karjavin, G. Kozlov, A. Lanev, P. Moisenz, V. Palichik, V. Perelygin, S. Shmatov, V. Smirnov, A. Volodko, A. Zarubin

Petersburg Nuclear Physics Institute, Gatchina (St Petersburg), Russia

V. Golovtsov, Y. Ivanov, V. Kim, P. Levchenko, V. Murzin, V. Oreshkin, I. Smirnov, V. Sulimov, L. Uvarov, S. Vavilov, A. Vorobyev, An. Vorobyev

Institute for Nuclear Research, Moscow, Russia

Yu. Andreev, A. Dermenev, S. Gninenko, N. Golubev, M. Kirsanov, N. Krasnikov, V. Matveev, A. Pashenkov, A. Toropin, S. Troitsky

Institute for Theoretical and Experimental Physics, Moscow, Russia

V. Epshteyn, M. Erofeeva, V. Gavrilo, V. Kaftanov[†], M. Kossov¹, A. Krokhotin, N. Lychkovskaya, V. Popov, G. Safronov, S. Semenov, V. Stolin, E. Vlasov, A. Zhokin

Moscow State University, Moscow, Russia

A. Belyaev, E. Boos, M. Dubinin³, L. Dudko, A. Ershov, A. Gribushin, O. Kodolova, I. Lokhtin, A. Markina, S. Obraztsov, M. Perfilov, S. Petrushanko, L. Sarycheva, V. Savrin, A. Snigirev

P.N. Lebedev Physical Institute, Moscow, Russia

V. Andreev, M. Azarkin, I. Dremin, M. Kirakosyan, A. Leonidov, G. Mesyats, S.V. Rusakov, A. Vinogradov

State Research Center of Russian Federation, Institute for High Energy Physics, Protvino, Russia

I. Azhgirey, I. Bayshev, S. Bitioukov, V. Grishin¹, V. Kachanov, D. Konstantinov, A. Korablev, V. Krychkine, V. Petrov, R. Ryutin, A. Sobol, L. Tourtchanovitch, S. Troshin, N. Tyurin, A. Uzunian, A. Volkov

University of Belgrade, Faculty of Physics and Vinca Institute of Nuclear Sciences, Belgrade, Serbia

P. Adzic²⁵, M. Djordjevic, D. Krpic²⁵, J. Milosevic

Centro de Investigaciones Energéticas Medioambientales y Tecnológicas (CIEMAT), Madrid, Spain

M. Aguilar-Benitez, J. Alcaraz Maestre, P. Arce, C. Battilana, E. Calvo, M. Cerrada, M. Chamizo Llatas, N. Colino, B. De La Cruz, A. Delgado Peris, C. Diez Pardos, D. Domínguez Vázquez, C. Fernandez Bedoya, J.P. Fernández Ramos, A. Ferrando, J. Flix, M.C. Fouz, P. Garcia-Abia, O. Gonzalez Lopez, S. Goy Lopez, J.M. Hernandez, M.I. Josa, G. Merino, J. Puerta Pelayo, I. Redondo, L. Romero, J. Santaolalla, M.S. Soares, C. Willmott

Universidad Autónoma de Madrid, Madrid, Spain

C. Albajar, G. Codispoti, J.F. de Trocóniz

Universidad de Oviedo, Oviedo, Spain

J. Cuevas, J. Fernandez Menendez, S. Folgueras, I. Gonzalez Caballero, L. Lloret Iglesias, J.M. Vizan Garcia

Instituto de Física de Cantabria (IFCA), CSIC-Universidad de Cantabria, Santander, Spain

J.A. Brochero Cifuentes, I.J. Cabrillo, A. Calderon, S.H. Chuang, J. Duarte Campderros, M. Felcini²⁶, M. Fernandez, G. Gomez, J. Gonzalez Sanchez, C. Jorda, P. Lobelle Pardo, A. Lopez Virto, J. Marco, R. Marco, C. Martinez Rivero, F. Matorras, F.J. Munoz Sanchez, J. Piedra Gomez²⁷, T. Rodrigo, A.Y. Rodríguez-Marrero, A. Ruiz-Jimeno, L. Scodellaro, M. Sobron Sanudo, I. Vila, R. Vilar Cortabitarte

CERN, European Organization for Nuclear Research, Geneva, Switzerland

D. Abbaneo, E. Auffray, G. Auzinger, P. Baillon, A.H. Ball, D. Barney, A.J. Bell²⁸, D. Benedetti, C. Bernet⁴, W. Bialas, P. Bloch, A. Bocci, S. Bolognesi, M. Bona, H. Breuker, K. Bunkowski, T. Camporesi, G. Cerminara, T. Christiansen, J.A. Coarasa Perez, B. Curé, D. D'Enterria, A. De Roeck, S. Di Guida, N. Dupont-Sagorin, A. Elliott-Peisert, B. Frisch, W. Funk, A. Gaddi, G. Georgiou, H. Gerwig, D. Gigi, K. Gill, D. Giordano, F. Glege, R. Gomez-Reino Garrido, M. Gouzevitch, P. Govoni, S. Gowdy, R. Guida, L. Guiducci, M. Hansen, C. Hartl, J. Harvey, J. Hegeman, B. Hegner, H.F. Hoffmann, V. Innocente, P. Janot, K. Kaadze, E. Karavakis, P. Lecoq, P. Lenzi, C. Lourenço, T. Mäki, M. Malberti, L. Malgeri, M. Mannelli, L. Masetti, A. Maurisset, G. Mavromanolakis, F. Meijers, S. Mersi, E. Meschi, R. Moser, M.U. Mozer, M. Mulders, E. Nesvold, M. Nguyen, T. Orimoto, L. Orsini, E. Palencia Cortezon, E. Perez, A. Petrilli, A. Pfeiffer, M. Pierini, M. Pimiä, D. Piparo, G. Polese, L. Quertenmont, A. Racz, W. Reece, J. Rodrigues Antunes, G. Rolandi²⁹, T. Rommerskirchen, C. Rovelli³⁰, M. Rovere, H. Sakulin, C. Schäfer, C. Schwick, I. Segoni, A. Sharma, P. Siegrist, P. Silva, M. Simon, P. Sphicas³¹, D. Spiga, M. Spiropulu³, M. Stoye, A. Tsirou, P. Vichoudis, H.K. Wöhri, S.D. Worm³², W.D. Zeuner

Paul Scherrer Institut, Villigen, Switzerland

W. Bertl, K. Deiters, W. Erdmann, K. Gabathuler, R. Horisberger, Q. Ingram, H.C. Kaestli, S. König, D. Kotlinski, U. Langenegger, F. Meier, D. Renker, T. Rohe, J. Sibille³³

Institute for Particle Physics, ETH Zurich, Zurich, Switzerland

L. Bäni, P. Bortignon, L. Caminada³⁴, B. Casal, N. Chanon, Z. Chen, S. Cittolin, G. Dissertori, M. Dittmar, J. Eugster, K. Freudenreich, C. Grab, W. Hintz, P. Lecomte, W. Luster-mann, C. Marchica³⁴, P. Martinez Ruiz del Arbol, P. Milenovic³⁵, F. Moortgat, C. Nägeli³⁴,

P. Nef, F. Nessi-Tedaldi, L. Pape, F. Pauss, T. Punz, A. Rizzi, F.J. Ronga, M. Rossini, L. Sala, A.K. Sanchez, M.-C. Sawley, A. Starodumov³⁶, B. Stieger, M. Takahashi, L. Tauscher[†], A. Thea, K. Theofilatos, D. Treille, C. Urscheler, R. Wallny, M. Weber, L. Wehrli, J. Weng

Universität Zürich, Zurich, Switzerland

E. Aguilo, C. Amsler, V. Chiochia, S. De Visscher, C. Favaro, M. Ivova Rikova, A. Jaeger, B. Millan Mejias, P. Otiougova, P. Robmann, A. Schmidt, H. Snoek

National Central University, Chung-Li, Taiwan

Y.H. Chang, K.H. Chen, C.M. Kuo, S.W. Li, W. Lin, Z.K. Liu, Y.J. Lu, D. Mekterovic, R. Volpe, S.S. Yu

National Taiwan University (NTU), Taipei, Taiwan

P. Bartalini, P. Chang, Y.H. Chang, Y.W. Chang, Y. Chao, K.F. Chen, C. Dietz, U. Grundler, W.-S. Hou, Y. Hsiung, K.Y. Kao, Y.J. Lei, R.-S. Lu, J.G. Shiu, Y.M. Tzeng, X. Wan, M. Wang

Cukurova University, Adana, Turkey

A. Adiguzel, M.N. Bakirci³⁷, S. Cerci³⁸, C. Dozen, I. Dumanoglu, E. Eskut, S. Girgis, G. Gokbulut, I. Hos, E.E. Kangal, A. Kayis Topaksu, G. Onengut, K. Ozdemir, S. Ozturk³⁹, A. Polatoz, K. Sogut⁴⁰, D. Sunar Cerci³⁸, B. Tali³⁸, H. Topakli³⁷, D. Uzun, L.N. Vergili, M. Vergili

Middle East Technical University, Physics Department, Ankara, Turkey

I.V. Akin, T. Aliev, B. Bilin, S. Bilmis, M. Deniz, H. Gamsizkan, A.M. Guler, K. Ocalan, A. Ozpineci, M. Serin, R. Sever, U.E. Surat, M. Yalvac, E. Yildirim, M. Zeyrek

Bogazici University, Istanbul, Turkey

M. Deliomeroglu, D. Demir⁴¹, E. Gülmez, B. Isildak, M. Kaya⁴², O. Kaya⁴², M. Özbek, S. Ozkorucuklu⁴³, N. Sonmez⁴⁴

National Scientific Center, Kharkov Institute of Physics and Technology, Kharkov, Ukraine

L. Levchuk

University of Bristol, Bristol, United Kingdom

F. Bostock, J.J. Brooke, T.L. Cheng, E. Clement, D. Cussans, R. Frazier, J. Goldstein, M. Grimes, G.P. Heath, H.F. Heath, L. Kreczko, S. Metson, D.M. Newbold³², K. Nirunpong, A. Poll, S. Senkin, V.J. Smith

Rutherford Appleton Laboratory, Didcot, United Kingdom

L. Basso⁴⁵, K.W. Bell, A. Belyaev⁴⁵, C. Brew, R.M. Brown, B. Camanzi, D.J.A. Cockerill, J.A. Coughlan, K. Harder, S. Harper, J. Jackson, B.W. Kennedy, E. Olaiya, D. Petyt, B.C. Radburn-Smith, C.H. Shepherd-Themistocleous, I.R. Tomalin, W.J. Womersley

Imperial College, London, United Kingdom

R. Bainbridge, G. Ball, J. Ballin, R. Beuselinck, O. Buchmuller, D. Colling, N. Cripps, M. Cutajar, G. Davies, M. Della Negra, W. Ferguson, J. Fulcher, D. Futyan, A. Gilbert, A. Guneratne Bryer, G. Hall, Z. Hatherell, J. Hays, G. Iles, M. Jarvis, G. Karapostoli, L. Lyons, A.-M. Magnan, J. Marrouche, B. Mathias, R. Nandi, J. Nash, A. Nikitenko³⁶, A. Papageorgiou, M. Pesaresi, K. Petridis, M. Pioppi⁴⁶, D.M. Raymond, S. Rogerson, N. Rompotis, A. Rose, M.J. Ryan, C. Seez,

P. Sharp, A. Sparrow, A. Tapper, S. Tourneur, M. Vazquez Acosta, T. Virdee, S. Wakefield, N. Wardle, D. Wardrope, T. Whyntie

Brunel University, Uxbridge, United Kingdom

M. Barrett, M. Chadwick, J.E. Cole, P.R. Hobson, A. Khan, P. Kyberd, D. Leslie, W. Martin, I.D. Reid, L. Teodorescu

Baylor University, Waco, U.S.A.

K. Hatakeyama, H. Liu

The University of Alabama, Tuscaloosa, U.S.A.

C. Henderson

Boston University, Boston, U.S.A.

T. Bose, E. Carrera Jarrin, C. Fantasia, A. Heister, J. St. John, P. Lawson, D. Lazic, J. Rohlf, D. Sperka, L. Sulak

Brown University, Providence, U.S.A.

A. Avetisyan, S. Bhattacharya, J.P. Chou, D. Cutts, A. Ferapontov, U. Heintz, S. Jabeen, G. Kukartsev, G. Landsberg, M. Luk, M. Narain, D. Nguyen, M. Segala, T. Sinthuprasith, T. Speer, K.V. Tsang

University of California, Davis, Davis, U.S.A.

R. Breedon, G. Breto, M. Calderon De La Barca Sanchez, S. Chauhan, M. Chertok, J. Conway, R. Conway, P.T. Cox, J. Dolen, R. Erbacher, R. Houtz, W. Ko, A. Kopecky, R. Lander, H. Liu, O. Mall, S. Maruyama, T. Miceli, M. Nikolic, D. Pellett, J. Robles, B. Rutherford, S. Salur, M. Searle, J. Smith, M. Squires, M. Tripathi, R. Vasquez Sierra

University of California, Los Angeles, Los Angeles, U.S.A.

V. Andreev, K. Arisaka, D. Cline, R. Cousins, A. Deisher, J. Duris, S. Erhan, C. Farrell, J. Hauser, M. Ignatenko, C. Jarvis, C. Plager, G. Rakness, P. Schlein[†], J. Tucker, V. Valuev

University of California, Riverside, Riverside, U.S.A.

J. Babb, R. Clare, J. Ellison, J.W. Gary, F. Giordano, G. Hanson, G.Y. Jeng, S.C. Kao, H. Liu, O.R. Long, A. Luthra, H. Nguyen, S. Paramesvaran, J. Sturdy, S. Sumowidagdo, R. Wilken, S. Wimpenny

University of California, San Diego, La Jolla, U.S.A.

W. Andrews, J.G. Branson, G.B. Cerati, D. Evans, F. Golf, A. Holzner, R. Kelley, M. Lebourgeois, J. Letts, B. Mangano, S. Padhi, C. Palmer, G. Petrucciani, H. Pi, M. Pieri, R. Ranieri, M. Sani, V. Sharma, S. Simon, E. Sudano, M. Tadel, Y. Tu, A. Vartak, S. Wasserbaech⁴⁷, F. Würthwein, A. Yagil, J. Yoo

University of California, Santa Barbara, Santa Barbara, U.S.A.

D. Barge, R. Bellan, C. Campagnari, M. D'Alfonso, T. Danielson, K. Flowers, P. Geffert, J. Incandela, C. Justus, P. Kalavase, S.A. Koay, D. Kovalskyi¹, V. Krutelyov, S. Lowette, N. Mccoll, S.D. Mullin, V. Pavlunin, F. Rebassoo, J. Ribnik, J. Richman, R. Rossin, D. Stuart, W. To, J.R. Vlimant, C. West

California Institute of Technology, Pasadena, U.S.A.

A. Apresyan, A. Bornheim, J. Bunn, Y. Chen, J. Duarte, M. Gataullin, Y. Ma, A. Mott, H.B. Newman, C. Rogan, K. Shin, V. Timciuc, P. Traczyk, J. Veverka, R. Wilkinson, Y. Yang, R.Y. Zhu

Carnegie Mellon University, Pittsburgh, U.S.A.

B. Akgun, R. Carroll, T. Ferguson, Y. Iiyama, D.W. Jang, S.Y. Jun, Y.F. Liu, M. Paulini, J. Russ, H. Vogel, I. Vorobiev

University of Colorado at Boulder, Boulder, U.S.A.

J.P. Cumalat, M.E. Dinardo, B.R. Drell, C.J. Edelmaier, W.T. Ford, A. Gaz, B. Heyburn, E. Luiggi Lopez, U. Nauenberg, J.G. Smith, K. Stenson, K.A. Ulmer, S.R. Wagner, S.L. Zang

Cornell University, Ithaca, U.S.A.

L. Agostino, J. Alexander, A. Chatterjee, N. Eggert, L.K. Gibbons, B. Heltsley, W. Hopkins, A. Khukhunaishvili, B. Kreis, G. Nicolas Kaufman, J.R. Patterson, D. Puigh, A. Ryd, E. Salvati, X. Shi, W. Sun, W.D. Teo, J. Thom, J. Thompson, J. Vaughan, Y. Weng, L. Winstrom, P. Wittich

Fairfield University, Fairfield, U.S.A.

A. Biselli, G. Cirino, D. Winn

Fermi National Accelerator Laboratory, Batavia, U.S.A.

S. Abdullin, M. Albrow, J. Anderson, G. Apollinari, M. Atac, J.A. Bakken, L.A.T. Bauerdick, A. Beretvas, J. Berryhill, P.C. Bhat, I. Bloch, K. Burkett, J.N. Butler, V. Chetluru, H.W.K. Cheung, F. Chlebana, S. Cihangir, W. Cooper, D.P. Eartly, V.D. Elvira, S. Esen, I. Fisk, J. Freeman, Y. Gao, E. Gottschalk, D. Green, O. Gutsche, J. Hanlon, R.M. Harris, J. Hirschauer, B. Hooberman, H. Jensen, S. Jindariani, M. Johnson, U. Joshi, B. Klima, K. Kousouris, S. Kunori, S. Kwan, C. Leonidopoulos, P. Limon, D. Lincoln, R. Lipton, J. Lykken, K. Maeshima, J.M. Marraffino, D. Mason, P. McBride, T. Miao, K. Mishra, S. Mrenna, Y. Musienko⁴⁸, C. Newman-Holmes, V. O'Dell, J. Pivarski, R. Pordes, O. Prokofyev, T. Schwarz, E. Sexton-Kennedy, S. Sharma, W.J. Spalding, L. Spiegel, P. Tan, L. Taylor, S. Tkaczyk, L. Uplegger, E.W. Vaandering, R. Vidal, J. Whitmore, W. Wu, F. Yang, F. Yumiceva, J.C. Yun

University of Florida, Gainesville, U.S.A.

D. Acosta, P. Avery, D. Bourilkov, M. Chen, S. Das, M. De Gruttola, G.P. Di Giovanni, D. Dobur, A. Drozdetskiy, R.D. Field, M. Fisher, Y. Fu, I.K. Furic, J. Gartner, S. Goldberg, J. Hugon, B. Kim, J. Konigsberg, A. Korytov, A. Kropivnitskaya, T. Kypreos, J.F. Low, K. Matchev, G. Mitselmakher, L. Muniz, P. Myeonghun, R. Remington, A. Rinkevicius, M. Schmitt, B. Scurlock, P. Sellers, N. Skhirtladze, M. Snowball, D. Wang, J. Yelton, M. Zakaria

Florida International University, Miami, U.S.A.

V. Gaultney, L.M. Lebolo, S. Linn, P. Markowitz, G. Martinez, J.L. Rodriguez

Florida State University, Tallahassee, U.S.A.

T. Adams, A. Askew, J. Bochenek, J. Chen, B. Diamond, S.V. Gleyzer, J. Haas, S. Hagopian, V. Hagopian, M. Jenkins, K.F. Johnson, H. Prosper, S. Sekmen, V. Veeraraghavan

Florida Institute of Technology, Melbourne, U.S.A.

M.M. Baarmand, B. Dorney, M. Hohlmann, H. Kalakhety, I. Vodopiyanov

University of Illinois at Chicago (UIC), Chicago, U.S.A.

M.R. Adams, I.M. Anghel, L. Apanasevich, Y. Bai, V.E. Bazterra, R.R. Betts, J. Callner, R. Cavanaugh, C. Dragoiu, L. Gauthier, C.E. Gerber, D.J. Hofman, S. Khalatyan, G.J. Kunde⁴⁹, F. Lacroix, M. Malek, C. O'Brien, C. Silkworth, C. Silvestre, A. Smoron, D. Strom, N. Varelas

The University of Iowa, Iowa City, U.S.A.

U. Akgun, E.A. Albayrak, B. Bilki, W. Clarida, F. Duru, C.K. Lae, E. McCliment, J.-P. Merlo, H. Mermerkaya⁵⁰, A. Mestvirishvili, A. Moeller, J. Nachtman, C.R. Newsom, E. Norbeck, J. Olson, Y. Onel, F. Ozok, S. Sen, J. Wetzel, T. Yetkin, K. Yi

Johns Hopkins University, Baltimore, U.S.A.

B.A. Barnett, B. Blumenfeld, A. Bonato, C. Eskew, D. Fehling, G. Giurgiu, A.V. Gritsan, Z.J. Guo, G. Hu, P. Maksimovic, S. Rappoccio, M. Swartz, N.V. Tran, A. Whitbeck

The University of Kansas, Lawrence, U.S.A.

P. Baringer, A. Bean, G. Benelli, O. Grachov, R.P. Kenny Iii, M. Murray, D. Noonan, S. Sanders, R. Stringer, J.S. Wood, V. Zhukova

Kansas State University, Manhattan, U.S.A.

A.F. Barfuss, T. Bolton, I. Chakaberia, A. Ivanov, S. Khalil, M. Makouski, Y. Maravin, S. Shrestha, I. Svintradze

Lawrence Livermore National Laboratory, Livermore, U.S.A.

J. Gronberg, D. Lange, D. Wright

University of Maryland, College Park, U.S.A.

A. Baden, M. Boutemur, S.C. Eno, D. Ferencek, J.A. Gomez, N.J. Hadley, R.G. Kellogg, M. Kirn, Y. Lu, A.C. Mignerey, K. Rossato, P. Rumerio, F. Santanastasio, A. Skuja, J. Temple, M.B. Tonjes, S.C. Tonwar, E. Twedt

Massachusetts Institute of Technology, Cambridge, U.S.A.

B. Alver, G. Bauer, J. Bendavid, W. Busza, E. Butz, I.A. Cali, M. Chan, V. Dutta, P. Everaerts, G. Gomez Ceballos, M. Goncharov, K.A. Hahn, P. Harris, Y. Kim, M. Klute, Y.-J. Lee, W. Li, C. Loizides, P.D. Luckey, T. Ma, S. Nahn, C. Paus, D. Ralph, C. Roland, G. Roland, M. Rudolph, G.S.F. Stephans, F. Stöckli, K. Sumorok, K. Sung, D. Velicanu, E.A. Wenger, R. Wolf, B. Wyslouch, S. Xie, M. Yang, Y. Yilmaz, A.S. Yoon, M. Zanetti

University of Minnesota, Minneapolis, U.S.A.

S.I. Cooper, P. Cushman, B. Dahmes, A. De Benedetti, G. Franzoni, A. Gude, J. Haupt, K. Klapoetke, Y. Kubota, J. Mans, N. Pastika, V. Rekovic, R. Rusack, M. Sasseville, A. Singovsky, N. Tambe, J. Turkewitz

University of Mississippi, University, U.S.A.

L.M. Cremaldi, R. Godang, R. Kroeger, L. Perera, R. Rahmat, D.A. Sanders, D. Summers

University of Nebraska-Lincoln, Lincoln, U.S.A.

K. Bloom, S. Bose, J. Butt, D.R. Claes, A. Dominguez, M. Eads, P. Jindal, J. Keller, T. Kelly, I. Kravchenko, J. Lazo-Flores, H. Malbouisson, S. Malik, G.R. Snow

State University of New York at Buffalo, Buffalo, U.S.A.

U. Baur, A. Godshalk, I. Iashvili, S. Jain, A. Kharchilava, A. Kumar, K. Smith, Z. Wan

Northeastern University, Boston, U.S.A.

G. Alverson, E. Barberis, D. Baumgartel, O. Boeriu, M. Chasco, S. Reucroft, J. Swain, D. Trocino, D. Wood, J. Zhang

Northwestern University, Evanston, U.S.A.

A. Anastassov, A. Kubik, N. Mucia, N. Odell, R.A. Ofierzynski, B. Pollack, A. Pozdnyakov, M. Schmitt, S. Stoynev, M. Velasco, S. Won

University of Notre Dame, Notre Dame, U.S.A.

L. Antonelli, D. Berry, A. Brinkerhoff, M. Hildreth, C. Jessop, D.J. Karmgard, J. Kolb, T. Kolberg, K. Lannon, W. Luo, S. Lynch, N. Marinelli, D.M. Morse, T. Pearson, R. Ruchti, J. Slaunwhite, N. Valls, M. Wayne, J. Ziegler

The Ohio State University, Columbus, U.S.A.

B. Bylsma, L.S. Durkin, C. Hill, P. Killewald, K. Kotov, T.Y. Ling, M. Rodenburg, C. Vuosalo, G. Williams

Princeton University, Princeton, U.S.A.

N. Adam, E. Berry, P. Elmer, D. Gerbaudo, V. Halyo, P. Hebda, A. Hunt, E. Laird, D. Lopes Pegna, D. Marlow, T. Medvedeva, M. Mooney, J. Olsen, P. Piroué, X. Quan, B. Safdi, H. Saka, D. Stickland, C. Tully, J.S. Werner, A. Zuranski

University of Puerto Rico, Mayaguez, U.S.A.

J.G. Acosta, X.T. Huang, A. Lopez, H. Mendez, S. Oliveros, J.E. Ramirez Vargas, A. Zatserklyaniy

Purdue University, West Lafayette, U.S.A.

E. Alagoz, V.E. Barnes, G. Bolla, L. Borrello, D. Bortoletto, M. De Mattia, A. Everett, L. Gutay, Z. Hu, M. Jones, O. Koybasi, M. Kress, A.T. Laasanen, N. Leonardo, V. Maroussov, P. Merkel, D.H. Miller, N. Neumeister, I. Shipsey, D. Silvers, A. Svyatkovskiy, M. Vidal Marono, H.D. Yoo, J. Zablocki, Y. Zheng

Purdue University Calumet, Hammond, U.S.A.

S. Guragain, N. Parashar

Rice University, Houston, U.S.A.

A. Adair, C. Boulahouache, K.M. Ecklund, F.J.M. Geurts, B.P. Padley, R. Redjimi, J. Roberts, J. Zabel

University of Rochester, Rochester, U.S.A.

B. Betchart, A. Bodek, Y.S. Chung, R. Covarelli, P. de Barbaro, R. Demina, Y. Eshaq, H. Flacher, A. Garcia-Bellido, P. Goldenzweig, Y. Gotra, J. Han, A. Harel, D.C. Miner, G. Petrillo, W. Sakumoto, D. Vishnevskiy, M. Zielinski

The Rockefeller University, New York, U.S.A.

A. Bhatti, R. Ciesielski, L. Demortier, K. Goulianos, G. Lungu, S. Malik, C. Mesropian

Rutgers, the State University of New Jersey, Piscataway, U.S.A.

S. Arora, O. Atramentov, A. Barker, C. Contreras-Campana, E. Contreras-Campana, D. Duggan, Y. Gershtein, R. Gray, E. Halkiadakis, D. Hidas, D. Hits, A. Lath, S. Panwalkar, M. Park, R. Patel, A. Richards, K. Rose, S. Schnetzer, S. Somalwar, R. Stone, S. Thomas

University of Tennessee, Knoxville, U.S.A.

G. Cerizza, M. Hollingsworth, S. Spanier, Z.C. Yang, A. York

Texas A&M University, College Station, U.S.A.

R. Eusebi, W. Flanagan, J. Gilmore, A. Gurrola, T. Kamon, V. Khotilovich, R. Montalvo, I. Osipenkov, Y. Pakhotin, A. Perloff, J. Roe, A. Safonov, S. Sengupta, I. Suarez, A. Tatarinov, D. Toback

Texas Tech University, Lubbock, U.S.A.

N. Akchurin, C. Bardak, J. Damgov, P.R. Duerdo, C. Jeong, K. Kovitanggoon, S.W. Lee, T. Libeiro, P. Mane, Y. Roh, A. Sill, I. Volobouev, R. Wigmans, E. Yazgan

Vanderbilt University, Nashville, U.S.A.

E. Appelt, E. Brownson, D. Engh, C. Florez, W. Gabella, M. Issah, W. Johns, C. Johnston, P. Kurt, C. Maguire, A. Melo, P. Sheldon, B. Snook, S. Tuo, J. Velkovska

University of Virginia, Charlottesville, U.S.A.

M.W. Arenton, M. Balazs, S. Boutle, B. Cox, B. Francis, S. Goadhouse, J. Goodell, R. Hirosky, A. Ledovskoy, C. Lin, C. Neu, J. Wood, R. Yohay

Wayne State University, Detroit, U.S.A.

S. Gollapinni, R. Harr, P.E. Karchin, C. Kottachchi Kankanamge Don, P. Lamichhane, M. Mattson, C. Milstène, A. Sakharov

University of Wisconsin, Madison, U.S.A.

M. Anderson, M. Bachtis, D. Belknap, J.N. Bellinger, D. Carlsmith, M. Cepeda, S. Dasu, J. Efron, E. Friis, L. Gray, K.S. Grogg, M. Grothe, R. Hall-Wilton, M. Herndon, A. Hervé, P. Klabbers, J. Klukas, A. Lanaro, C. Lazaridis, J. Leonard, R. Loveless, A. Mohapatra, I. Ojalvo, W. Parker, I. Ross, A. Savin, W.H. Smith, J. Swanson, M. Weinberg

†: Deceased

- 1: Also at CERN, European Organization for Nuclear Research, Geneva, Switzerland
- 2: Also at Universidade Federal do ABC, Santo Andre, Brazil
- 3: Also at California Institute of Technology, Pasadena, U.S.A.
- 4: Also at Laboratoire Leprince-Ringuet, Ecole Polytechnique, IN2P3-CNRS, Palaiseau, France
- 5: Also at Suez Canal University, Suez, Egypt
- 6: Also at Cairo University, Cairo, Egypt
- 7: Also at British University, Cairo, Egypt
- 8: Also at Fayoum University, El-Fayoum, Egypt
- 9: Also at Ain Shams University, Cairo, Egypt
- 10: Also at Soltan Institute for Nuclear Studies, Warsaw, Poland
- 11: Also at Université de Haute-Alsace, Mulhouse, France
- 12: Also at Moscow State University, Moscow, Russia
- 13: Also at Brandenburg University of Technology, Cottbus, Germany
- 14: Also at Institute of Nuclear Research ATOMKI, Debrecen, Hungary
- 15: Also at Eötvös Loránd University, Budapest, Hungary
- 16: Also at Tata Institute of Fundamental Research - HECR, Mumbai, India
- 17: Also at University of Visva-Bharati, Santiniketan, India
- 18: Also at Sharif University of Technology, Tehran, Iran
- 19: Also at Isfahan University of Technology, Isfahan, Iran
- 20: Also at Shiraz University, Shiraz, Iran
- 21: Also at Facoltà Ingegneria Università di Roma, Roma, Italy
- 22: Also at Università della Basilicata, Potenza, Italy
- 23: Also at Laboratori Nazionali di Legnaro dell' INFN, Legnaro, Italy
- 24: Also at Università degli studi di Siena, Siena, Italy
- 25: Also at Faculty of Physics of University of Belgrade, Belgrade, Serbia
- 26: Also at University of California, Los Angeles, Los Angeles, U.S.A.
- 27: Also at University of Florida, Gainesville, U.S.A.
- 28: Also at Université de Genève, Geneva, Switzerland
- 29: Also at Scuola Normale e Sezione dell' INFN, Pisa, Italy
- 30: Also at INFN Sezione di Roma; Università di Roma "La Sapienza", Roma, Italy
- 31: Also at University of Athens, Athens, Greece
- 32: Now at Rutherford Appleton Laboratory, Didcot, United Kingdom
- 33: Also at The University of Kansas, Lawrence, U.S.A.
- 34: Also at Paul Scherrer Institut, Villigen, Switzerland
- 35: Also at University of Belgrade, Faculty of Physics and Vinca Institute of Nuclear Sciences, Belgrade, Serbia
- 36: Also at Institute for Theoretical and Experimental Physics, Moscow, Russia
- 37: Also at Gaziosmanpasa University, Tokat, Turkey
- 38: Also at Adiyaman University, Adiyaman, Turkey
- 39: Also at The University of Iowa, Iowa City, U.S.A.
- 40: Also at Mersin University, Mersin, Turkey
- 41: Also at Izmir Institute of Technology, Izmir, Turkey
- 42: Also at Kafkas University, Kars, Turkey
- 43: Also at Suleyman Demirel University, Isparta, Turkey
- 44: Also at Ege University, Izmir, Turkey
- 45: Also at School of Physics and Astronomy, University of Southampton, Southampton, United Kingdom
- 46: Also at INFN Sezione di Perugia; Università di Perugia, Perugia, Italy
- 47: Also at Utah Valley University, Orem, U.S.A.
- 48: Also at Institute for Nuclear Research, Moscow, Russia
- 49: Also at Los Alamos National Laboratory, Los Alamos, U.S.A.
- 50: Also at Erzincan University, Erzincan, Turkey